ACM Siggraph*Asia*2009 - Course Notes

Biophysically-Based Appearance Models:
The Bumpy Road Toward Predictability

Presenter:
Gladimir V. G. Baranoski
Natural Phenomena Simulation Group
School of Computer Science
University of Waterloo
200 University Avenue West
Waterloo, Ontario, Canada, N2L 3G1
Email: gvgbaran@curumin.cs.uwaterloo.ca

Yokohama, Japan, December 2009

Contents

Course Description

The main purpose of this course is to address practical issues involved in the development of biophysically-based light transport models used to simulate the appearance of natural materials. Furthermore, since these models are used not only in image synthesis, but also in other scientific applications (e.g., noninvasive diagnosis of medical conditions and remote sensing of natural resources), it also aims to foster the cross-fertilization between computer graphics and these fields by identifying common needs and complementary resources. The course begins by providing a concise review of relevant biophysical background, followed by a discussion on the key concept of predictability. It continues by examining the specific constraints and pitfalls found in each of the key stages of the simulation framework, namely data collection, modeling and evaluation, and discussing alternatives to improve the fidelity of the entire process. Once a model is designed, implemented and evaluated through a sound methodology, its scope of applications can be expanded to address a wide range of scientific questions. For example, computer simulations are regularly being used by life science researchers to understand and predict material appearance changes prompted by mechanisms which cannot be fully studied using traditional experimental procedures. In line with this trend, the course closes with an examination of recent examples of computer graphics appearance models which can also be employed in such interdisciplinary research efforts.

Prerequisites

This course assumes a familiarity with basic optics concepts and radiometric terms. Participants should have a working knowledge of standard rendering techniques and terminology. Experience with Monte Carlo methods is helpful, but not required.

Presenter's Short Biography

Gladimir V. G. Baranoski received a Ph.D. in Computer Science from the University of Calgary in 1998. Currently, he is an Associate Professor at the School of Computer Science and the leader of the Natural Phenomena Simulation Group at the University of Waterloo, Canada. His current research interests include the predictive simulation of light interactions with organic and inorganic materials and the biophysically-based rendering of natural phenomena. The results of his multidisciplinary research on the modeling of light interactions with natural materials (*e.g.*, plants, soil and human tissues) have been made available to the scientific community through the publication of articles in journals and conference proceedings in computer graphics and related fields such as applied optics and remote sensing. He has organized and presented several courses in computer graphics conferences (*e.g.*, Eurographics (2001, 2002 and 2005), Siggraph (2002 and 2003), Siggraph Asia (2008)) and remote sensing symposiums (*e.g.*, The 9th International Symposium on Physical Measurements and Signatures in Remote Sensing - ISPMSRS 2005, and The IEEE International Geoscience and Remote Sensing Symposium - IGARSS 2008 and IGARSS 2009).

Further information about the presenter can be found at:
$http://www.npsg.uwaterloo.ca/people/gladimir/$

Course Extended Summary

In 1987, in his Steven Coons Award lecture, Greenberg [28] stated:

> *If computer graphics is to have a role in improving the future of our civilization, the real value will be in its application to science, engineering and design.*

More than two decades have passed since then, and one wonders whether or not this statement is being completely fulfilled. There is no doubt that computer graphics has provided valuable contributions to many fields. For instance, realistic image synthesis frameworks are being extensively used in the automotive industry and architectural projects. In fact, the current state of art in rendering allows us to generate images of a wide range of materials, specially man-made ones, which are oftentimes indistinguishable from their real counterparts. The question is: can we do more, *i.e.*, how far can we go beyond the rendering of images that look right, and what are the obstacles ahead?

One of the key components of image synthesis frameworks corresponds to the modeling of light and matter interactions, *i.e.*, how different materials reflect and transmit light so that they are assigned appropriate appearance attributes such as color, glossiness and translucency. Undeniably a significant progress has been achieved in this area. We have moved from ad hoc to physically-based models, and the impact on the realism of computer generated images was remarkable. Following up on this trend, graphics researchers started to look for computational solutions that would also lead to predictable results, specially for natural materials. To achieve this goal, the models need to be controlled by biophysically meaningful parameters, such as the type and concentration of the pigments found in the organic tissues, and carefully simulate the biophysical light propagation and absorption processes that determine material appearance attributes.

In the last decade, a number of models aiming at this goal have been proposed. Comprehensive [65] and specific [5] reviews of these models have been presented in recent graphics events. For this reason, these reviews are not repeated in this course which has a different purpose. It examines these modeling efforts from a scientific methodology point of view, *i.e.*, judiciously looking at the different stages of the simulation framework to point out practical and scientific issues usually overlooked by the existing simulation approaches. It builds on the interdisciplinary experience gained during the development of predictive light interaction models for different organic and inorganic materials, which is transparently shared with the attendees.

The course begins by providing an overview of the processes involved in the interactions of light with matter and a brief description of measurement of appearance concepts [38]. The key concept of predictability is then presented along with an outline of its potential benefits not only to rendering applications, but also to life sciences research. In order to develop such models, a scientifically sound methodology, involving data collection, modeling and evaluation, should be applied. Accordingly, the course continues by examining the limitations and problems that need to be tackled in each of these stages to improve the correctness of the existing models and to facilitate the design of new predictive models. This examination is illustrated by examples provided by state of the art models originally developed by graphics researchers and aimed not only to realistic rendering, but also to applications in other scientific fields such as remote sensing and applied optics.

It is a well known fact that a well designed model is of little use without reliable specimen characterization data to be used as input, and accurate evaluation data against which it can be compared [1, 81]. The specimen's characterization data corresponds to biophysical parameters, such as thickness, concentration of pigments and refractive indices, that affect the transport and absorption of light by organic materials. The evaluation data corresponds to the group of measurements that indicate the appearance of the material [38]. These measurements involve the spectral distribution (usually given in terms of reflectance and transmittance) and the spatial distribution (usually given in terms of BRDF and BTDF) of light propagated by the material. In order to evaluate the accuracy and predictability of a given model, one can compare modeled results with measured (evaluation) data. Ideally, the characterization data to be incorporated into the model should correspond to the specimen used to obtain the evaluation data. However, very few spectral data sets (*e.g.*, [36]) provide a detailed description of the properties of the specimens used in the radiometric measurements. In fact, for many materials, only averaged data is available in the scientific literature. The characterization data is even more scarce for materials in their pure form, such as natural chromophores, whose absorption profile is usually obtained either through inversion procedures (which may be biased by the inaccuracies of the inverted model) or does not take into account *in vivo* vs. *in vitro* effects [21]. Furthermore, although evaluation data, such as spectral reflectance and transmittance curves can be found in the scientific literature, they are usually restricted to a narrow range of measurement conditions. In terms of goniophotometric (BRDF and BTDF) curves, despite valuable measurement efforts [54], there is still a shortage of data, and usually the available data sets present the similar scope and range limitations outlined above for the spectral data sets. The lack of measured data is even more serious with respect to subsurface scattering data which, to the best of our knowledge, is available only for few tissue samples. In the data availability section of the course, we discuss these issues, and examine how they affect the predictability of the existing models and their evaluation.

For the sake of completeness and accuracy, one would like to take into account all of the structural and optical characteristics of a given material during the modeling stage. However, as outlined above, even if one is able to represent a material in a molecular level, data may not be available to support such a detailed description. Hence, researchers attempt to find an appropriate level of abstraction for the material at hand in order to balance data availability and accuracy issues. At one end of the spectrum, there are models which simulate light transport by geometrically representing the material's individual constituents (*e.g.*, cells [27]). At the other end, there are models that use the intuitive concept of layers in which the properties of the material's individual constituents are globally described through mathematical expressions (*e.g.*, using pre-computed analytical functions to represent the scattering of light within a given tissue [63]). Alternatively, as it was recently demonstrated [47], it is also possible to compute the light propagation profile within a tissue without resorting to neither of these approaches, *i.e.*, the directional changes are computed on the fly taking into account the geometrical characteristics of the material's individual constituents without explicitly storing them. No approach is superior for all materials, and regardless of the selected level of abstraction, simplifying assumptions and generalizations are usually employed in the current models due to practical constraints and the inherent complexity of natural materials. In the discussion regarding the modeling stage, we address these issues and discuss their impact on the efficacy of the existing simulation frameworks.

In order to claim that a model is predictive, one has to provide evidence of its correctness [30]. This makes the evaluation stage essential to determine the fidelity of a given model. Among the different evaluations approaches being employed in graphics, the visual inspection is arguably the most suitable if one is interested in the generation of believable images. It has limitations, however, when comes to assess the accuracy of a model since the final images are affected by other segments of the rendering pipeline (*e.g.*, geometrical modeling and spectral sampling). Another commonly used approach involves the comparison of modeled results with results provided by models designed for the same purpose. This approach has limitations as well. For example, for a given a material, it may not be possible to find an existing model which provides the same type of readings. Furthermore, even if such a model exists, the fact that the results of the model being evaluated and the readings provided by the reference model are in good agreement does not mean necessarily that both models are correct. In fact, it may be possible that both sets of readings are far from the actual values measured for the physical phenomena being simulated. A more reliable approach involves comparisons with the "real thing". These comparisons may be quantitative or qualitative. The first group involves direct (quantitative) comparisons of spectral (*e.g.*, reflectance and transmittance) and spatial (*e.g.*, BRDF and BTDF) measured values and modeled results. The second group refers to actual observations of a phenomenon behavior (*e.g.*, the presence of a characteristic oxygenated hemoglobin "W" signature in the reflectance of lightly pigmented skin specimens [48]), and whether or not the model can (qualitatively) reproduce it. As mentioned before, this approach is bound by data availability. However, by isolating the model from the rendering pipeline and comparing it with actual measurements, it mitigates the presence of biases in the evaluation process and facilitates the identification of model parameters and algorithms that are amenable to modification and correction. Hence, it more clearly signalizes the points that can be improved so that more accurate models can be designed for the material at hand.

Although the journey toward predictability has many hurdles, it can significantly contribute to the expansion of computer graphics boundaries, the ultimate challenge facing the graphics community as recently highlighted by Greenberg [29]. Viewed in this context, this journey offers several opportunities for synergistic collaborations between graphics researchers and scientists from other fields. For example, once a model is designed, implemented and evaluated through a sound methodology, it can be applied not only to visually assist scientists through the generation of predictable images of known phenomena, but also to provide a computational testing set up for the investigation of processes that cannot be studied through traditional experimental procedures. Eventually, such processes can be also incorporated into the model's formulation. To illustrate these points, the course closes with an overview of recent examples of models whose development followed this pattern. More importantly, this final component of the course emphasizes the idea that the pursue of predictability is an iterative effort, which itself can contribute to accelerate the hypothesis generation and validation cycles of research in different fields [79].

Syllabus and Schedule

1. Introduction [5min]

2. Biophysical Background [10min]
   2.1 Light and Matter Interactions
   2.2 Measurement of Appearance

3. Quest for Predictability [10min]
   3.1 What does it mean?
   3.2 Why is it useful?
   3.3 How it can be attained?

4. Data Availability [20min]
   4.1 Characterization Data Constraints
   4.2 Evaluation Data Constraints

5. Modeling Issues [20min]
   5.1 What's the appropriate level of abstraction?
   5.2 Simplifying Assumptions
   5.3 Unsound Generalizations

6. Evaluation Approaches [20min]

    6.1 Visual Inspection

    6.2 Collateral Comparisons

    6.3 Comparisons with the ”Real Thing”

7. Scientific Prospects [15min]

8. Concluding Remarks [5min]

Bibliography

[1] BARANOSKI, G. Modeling the interaction of infrared radiation (750 to 2500nm) with bifacial and unifacial plant leaves. *Remote Sensing of Environment 100* (2006), 335–347.

[2] BARANOSKI, G. On the predictive modeling of visible light interaction with fresh and environmentally stressed monocotyledonous leaves. In *International Geoscience and Remote Sensing Symposium - IGARSS'09* (Cape Town, South Africa, July 2009), IEEE. to appear.

[3] BARANOSKI, G., AND ENG, D. An investigation on sieve and detour effects affecting the interaction of collimated and diffuse infrared radiation (750 to 2500nm) with plant leaves. *IEEE Transactions on Geoscience and Remote Sensing 45* (2007), 2593–2599.

[4] BARANOSKI, G., AND KRISHNASWAMY, A. Simulation of light interaction with human skin. The Eurographics Association and The Image Synthesis Group, Dublin, Ireland, September 2005. Eurographics Tutorial 6.

[5] BARANOSKI, G., AND KRISHNASWAMY, A. Light interaction with human skin: From believable images to predictable models. In *Siggraph Asia (Singapore)* (Singapore, 2008). Course Notes.

[6] BARANOSKI, G., KRISHNASWAMY, A., AND KIMMEL, B. An investigation on the use of data-driven scatering profiles in Monte Carlo simulations of ultraviolet light propagation in skin tissues. *Physics in Medicine and Biology 49* (2004), 4799–4809.

[7] BARANOSKI, G., KRISHNASWAMY, A., AND KIMMEL, B. Increasing the predictability of tissue subsurface scattering simulations. *The Visual Computer 21*, 4 (May 2005), 265–278.

[8] BARANOSKI, G., AND LAM, M. Qualitative assessment of undetectable melanin distribution in lightly pigmented irides. *Journal of Biomedical Optics 12*, 3 (August 2007), (030501):1–3.

[9] BARANOSKI, G., AND ROKNE, J. An algorithmic reflectance and transmittance model for plant tissue. *Computer Graphics Forum 16*, 3 (1997), 141–150.

[10] BARANOSKI, G., AND ROKNE, J. *Light Interaction with Plants: A Computer Graphics Perspective*. Horwood Publishing, Chichester, UK, 2004.

[11] BARANOSKI, G., ROKNE, J., AND XU, G. Virtual spectrophotometric measurements for biologically and physically-based rendering. *The Visual Computer 17*, 8 (2001), 506–518.

[12] BELL, I., AND BARANOSKI, G. More than RGB: moving toward spectral color reproduction. ACM Siggraph Course Notes, San Diego, CA, July 2003. Course 24.

[13] BRULS, W., AND VAN DER LEUN, J. Forward scattering properties of human epidermal layers. *Photochem. Photobiol. 40* (1984), 231–242.

[14] CHEN, B., STAMNES, K., AND STAMNES, J. Validity of the diffusion approximation in bio-optical imaging. *Applied Optics 40*, 34 (2001), 6356–6336.

[15] CHEN, T., BARANOSKI, G., AND LIN, K. Bulk scattering approximations for HeNe laser transmitted through paper. *Optics Express 16*, 26 (2008), 21762–21771.

[16] CIE. *Colorimetry Official Recommendations of the International Commission on Illumination*. Commission Internationale de L'Eclairage (CIE), 1970.

[17] COULSON, K., G.M, B., AND GRAY, E. Optical reflection properties of natural surfaces. *Journal of Geophysical Research 70*, 18 (1965), 4601–4611.

[18] DICKEY, D., MOORE, R., AND TULIP, J. Using radiance predicted by the P3-Approximation in a spherical geometry to predict tissue optical properties. In *Clinical Lasers and Diagnostics* (2001), P. Brouwer, Ed., SPIE, vol. 4156, pp. 181–188.

[19] DORSEY, J., RUSHMEIER, H., AND SILLION, F. *Digital Modeling of Material Appearance*. Morgan Kaufmann/Elsevier, 2007.

[20] EAGLE, R. Iris pigmentation and pigmented lesions: an ultrastructural study. *Trans. Am. Ophthalmol. Soc. 88* (1988), 581–687.

[21] ENG, D. On the application of photoacoustic absorption spectral data to the modeling of leaf optical properties. Master's thesis, School of Computer Science, University of Waterloo, Waterloo, Canada, 2007.

[22] ENG, D., AND BARANOSKI, G. The application of photoacoustic absorption spectral data to the modeling of leaf optical properties in the visible range. *IEEE Transactions on Geoscience and Remote Sensing 45* (2007), 4077–4086.

[23] FARELL, T., PATTERSON, M., AND WILSON, B. A diffusion theory model of spatially resolved, steady-state diffuse reflectance for the noninvasive determination of tissue optical properties in vivo. *Medical Physics 19* (1992), 879–888.

[24] FARRANT, P. *Color in Nature: A Visual and Scientific Exploration*. Blandford Press, London, 1999.

[25] FITZPATRICK, T., AND BOLOGNIA, J. Human melanin pigmentation: role in pathogenesis of cutaneous melanoma. In *Melanin: Its Role in Human Photoprotection* (Overland Park, Kansas, USA, 1995), M. C. L. Zeise and T. Fitzpatrick, Eds., Valdenmar Publishing Company, pp. 177–182.

[26] GLASSNER, A. *Principles of Digital Image Synthesis*. Morgan Kaufmann Publishers, Inc, San Francisco, 1995.

[27] GOVAERTS, Y., JACQUEMOUD, S., VERSTRAETE, M., AND USTIN, S. Three-dimensional radiation transfer modeling in a dycotyledon leaf. *Applied Optics 35*, 33 (November 1996), 6585–6598.

[28] GREENBERG, D. 1987 Steven A. Coons Award Lecture. *Computer Graphics 22*, 1 (February 1988), 7–14.

[29] GREENBERG, D. The expanding boundaires of computer graphics. In *Siggraph Asia (Singapore)* (Singapore, 2008). Featured Speaker.

[30] GREENBERG, D., ARVO, J., LAFORTUNE, E., TORRANCE, K., FERWERDA, J., WALTER, B., TRUMBORE, B., SHIRLEY, P., PATTANAIK, S., AND FOO, S. A framework for realistic image synthesis. In *Siggraph, Annual Conference Series* (1997), pp. 477–494.

[31] GROSS, D. Report from the fidelity implementation study group. In *Simulation Interoperability Workshop, Simulation Interoperability and Standards Organization* (Orlando, FL, USA, 1999). Paper 99S-SIW-167.

[32] HANRAHAN, P., AND KRUEGER, W. Reflection from layered surfaces due to subsurface scattering. In *Siggraph, Annual Conference Series* (August 1993), pp. 165–174.

[33] HENYEY, L., AND GREENSTEIN, J. Diffuse radiation in the galaxy. *Astrophysics Journal 93* (1941), 70–83.

[34] HIELSCHER, A., ALCOUFFE, R., AND BARBOUR, R. Comparison of finite-difference transport and diffusion calculations for photon migration in homogeneous tissues. *Physics in Medicine and Biology 43* (1998), 1285–1302.

[35] HONG, S., SIMPSON, B., AND BARANOSKI, G. Interactive venation-based leaf shape modeling. *Computer Animation and Virtual Worlds 16* (2005), 415–427.

[36] HOSGOOD, B., JACQUEMOUD, S., ANDREOLI, G., VERDEBOUT, J., PEDRINI, G., AND SCHMUCK, G. Leaf optical properties experiment 93. Tech. Rep. Report EUR 16095 EN, European Comission, Joint Research Center, Institute for Remote Sensing Applications, Italy, 1995.

[37] HUDSON, E., STRINGER, M., CAIRNDUFF, F., ASH, D., AND SMITH, M. The optical properties of skin tumors measured during superficial photodynamic therapy. *Lasers in Medical Science 9* (1994), 99–103.

[38] HUNTER, R., AND HAROLD, R. *The Measurement of Appearance*, second ed. John Wiley & Sons, New York, 1987.

[39] IMESH, P., WALLOW, I., AND ALBERT, D. The color of the human eye: a review of morphological correlates and some conditions that affect iridal pigmentation. *Surv. Ophthalmol. 41*, 2 (1997), 117–123.

[40] ISHIMARU, A. *Wave Propagation and Scattering in Random Media*, 2nd ed., vol. 2. IEEE Press, New York, 1978.

[41] JACQUEMOUD, S., AND USTIN, S. Leaf optical properties: A state of the art. In *8th International Symposium of Physical Measurements & Signatures in Remote Sensing* (Aussois, France, January 2001), CNES, pp. 223–332.

[42] JACQUEMOUD, S., USTIN, S., VERDEBOUT, J., SCHMUCK, G., ANDREOLI, G., AND HOSGOOD, B. Estimating leaf biochemistry using prospect leaf optical properties model. *Remote Sensing of Environment 56* (1996), 194–202.

[43] JACQUES, S. Origins of tissue optical properties in the UVA visible and NIR regions. *OSA TOPS on Advances in Optical Imaging and Photon Migration 2* (1996), 364–369.

[44] JACQUES, S., ALTER, C., AND PRAHL, S. Angular dependence of HeNe laser light scattering by human dermis. *Lasers in Life Sciences 1*, 4 (1987), 309–333.

[45] JENSEN, H., MARSCHNER, S., LEVOY, M., AND HANRAHAN, P. A practical model for subsurface light transport. In *Siggraph, Annual Conference Series* (August 2001), pp. 511–518.

[46] KIMMEL, B. SPLITS: A spectral light transport model for sand. Master's thesis, School of Computer Science, University of Waterloo, Waterloo, Canada, 2005.

[47] KIMMEL, B., AND BARANOSKI, G. A novel approach for simulating light interaction with particulate materials: application to the modeling of sand spectral properties. *Optics Express 15*, 15 (2007), 9755–9777.

[48] KRISHNASWAMY, A., AND BARANOSKI, G. A biophysically-based spectral model of light interaction with human skin. *Computer Graphics Forum 23*, 3 (2004), 331–340.

[49] KRISHNASWAMY, A., BARANOSKI, G., AND ROKNE, J. G. Improving the reliability/cost ratio of goniophotometric measurements. *Journal of Graphics Tools 9*, 3 (2004), 31–51.

[50] LAM, M., AND BARANOSKI, G. A predictive light transport model for the human iris. *Computer Graphics Forum 25*, 3 (2006), 359–368.

[51] LI, Z., FUNG, A., TJUATJA, S., GIBBS, D., BETTY, C., AND IRONS, J. A modeling study of backscattering from soil surfaces. *IEEE Transactions on Geoscience and Remote Sensing 34*, 1 (January 1996), 264–271.

[52] LOBELL, D., AND ASNER, G. Moisture effects on soil reflectance. *Soil Science Society of America Journal 66*, 3 (May 2002), 722–727.

[53] MARACCI, G., SCHMUCK, G., HOSGOOD, B., AND ANDREOLI, G. Interpretation of reflectance spectra by plant physiological parameters. In *International Geoscience and Remote Sensing Symposium - IGARSS'91* (Espoo, Finland, 1991), pp. 2303–2306.

[54] MARSCHNER, S., WESTIN, S. H., LAFORTUNE, E., TORRANCE, K., AND GREENBERG, D. Image-based brdf measurement including human skin. In *Rendering Techniques'1999 (Proceedings of the 10th Eurographics Rendering Workshop)* (Granada, June 1999), D. Lischinski and G. W. Larson, Eds., Springer-Verlag, pp. 119–130.

[55] MINNAERT, M. *Light and Color in the Outdoors*. Springer-Verlag, New York, NY, 1993.

[56] MINORSKY, P. Achieving the *in silico* plant. Systems biology and the future of plant biological research. *Plant Physiology 132* (2003), 404–409.

[57] NAGEL, E., LICHTENTHALER, H., KOSCHANYL, L., AND BIACS, P. Photoacoustic spectra of chlorophylls and carotenoids in fruits and in plant oils. In *Biological Role of Plant Lipids* (New York, NY, U.S.A., 1989), P. Biacs, K. Guiz, and T. Kremmer, Eds., Plenum Publishing, pp. 271–273.

[58] NICODEMUS, F., RICHMOND, J., HSIA, J., GINSBERG, I., AND LIMPERIS, T. Geometrical considerations and nomenclature for reflectance. In *Physics-Based Vision Principles and Practice: Radiometry* (Boston, 1992), L. Wolff, S. Shafer, and G. Healey, Eds., Jones and Bartlett Publishers, pp. 94–145.

[59] NISCHIK, M., AND FORSTER, C. Analysis of skin erythema using true-color images. *IEEE Transactions on Medical Imaging 16*, 6 (December 1997), 711–716.

[60] PATHAK, M. Functions of melanin and protection by melanin. In *Melanin: Its Role in Human Photoprotection* (Overland Park, Kansas, USA, 1995), M. C. L. Zeise and T. Fitzpatrick, Eds., Valdenmar Publishing Company, pp. 125–134.

[61] POPOV, A., PRIEZZHEV, A., LADEMANN, J., AND MYLLYLÄ, R. TiO_2 nanoparticles as an effective UV-B radiation skin-protective compound in sunscreens. *Journal of Physics D: Applied Physics 38* (2005), 2564–2570.

[62] PRAHL, S. *Light Transport in Tissue*. PhD thesis, The University of Texas at Austin, TX, USA, December 1988.

[63] PRAHL, S., KEIJZER, M., JACQUES, S., AND WELCH, A. A Monte Carlo model of light propagation in tissue. *SPIE Institute Series IS 5* (1989), 102–111.

[64] RILEY, N. Projection sphericity. *Journal of Sedimentary Petrology 11*, 2 (1941), 94–95.

[65] RUSHMEIER, H., DORSEY, J., AND SILLION, F. Advanced material appearance modeling. In *Siggraph, Annual Conference Series* (Los Angeles, 2008). Course Notes.

[66] SARDAR, D., AND LEVY, L. Optical properties of whole blood. *Lasers in Medical Science 13* (1998), 106–111.

[67] SMITH, H., AND MORGAN, D. The spectral characteristics of the visible radiation incident upon the surface of the Earth. In *Plants and the Daylight Spectrum* (London, January 1981), H. Smith, Ed., Academic Press, pp. 3–20.

[68] SOKOLIK, I., AND TOON, O. Incorporation of mineralogical composition into models of the radiative properties of mineral aerosol from UV to IR wavelengths. *Journal of Geophysical Research 104*, D9 (April 1999), 9423–9444.

[69] STAR, W. Light dosimetry *in vivo*. *Physics in Medicine and Biology 42* (1997), 763–787.

[70] STEINKE, J., AND SHEPHERD, A. Diffusion model of the optical absorbance of whole blood. *Journal of the Optical Society of America 5*, 6 (1988), 813–822.

[71] TALREJA, P., KASTING, G., KLEENE, N., PICKENS, W., AND WANG, T. Visualization of the lipid barrier and measurement of lipid pathlength in human stratum corneum. *AAPS PharmSCi 3*, 2 (2001), 1–9.

[72] TEHRANI, H., WALLS, J., COTTON, S., SASSOON, E., AND HALL, P. Spectrophotometric intracutaneous analysis in the diagnosis of basl cell carcinoma: a pilot study. *International Journal of Dermatology 46* (2007), 371–375.

[73] THOMAS, J., NAMKEM, L., OERTHER, G., AND BROWN, R. Estimating leaf water content by reflectance measurements. *Agronomy Journal 63* (1971), 845–847.

[74] TUCHIN, V. *Tissue Optics Light Scattering Methods and Instruments for Medical Diagnosis*. The International Society for Optical Engineering, Bellingham, WA, USA, 2000.

[75] VAN DE HULST, H. *Multiple Light Scattering: Tables, Formulas, and Applications*, vol. 1. Academic Press, New York, 1980.

[76] VAN DE HULST, H. *Multiple Light Scattering: Tables, Formulas, and Applications*, vol. 2. Academic Press, New York, 1980.

[77] VAN DE HULST, H. *Light Scattering by Small Particles*, 2nd ed. Dover Publications Inc., New York, 1981.

[78] VAN GEMERT, M., JACQUES, S., STERENBORG, H., AND STAR, W. Skin optics. *IEEE Transactions on Biomedical Engineering 36*, 12 (1989), 1146–1154.

[79] VENTURA, B., LEMERLE, C., MICHALODIMITRAKIS, K., AND SERRANO, L. From *in vivo* to *in silico* biology and back. *Nature 443* (2006), 527–553.

[80] VRHEL, M., GERSHON, R., AND IWAN, L. Measurement and analysis of object reflectance spectra. *Color Research and Application 19*, 1 (1994), 4–9.

[81] WARD, G. Measuring and modeling anisotropic reflection. *Computer Graphics (Siggraph Proceedings)* (July 1992), 265–272.

[82] WIELGUS, A., AND SARNA, T. Melanin in human irides of different color and age of donors. *Pigment Cell Res. 18* (2005), 454–464.

[83] WILLIAMSON, S., AND CUMMINS, H. *Light and Color in Nature and Art*. John Wiley & Sons, New York, 1983.

[84] WOOLLEY, J. Reflectance and transmittance of light by leaves. *Plant Physiology 47* (1971), 656–662.

[85] WOOLLEY, J. Refractive index of soybean leaf cell walls. *Plant Physiology 55* (1975), 172–174.

[86] YAMAGUCHI, M., MITSUI, M., MURAKAMI, Y., FUKUDA, H., OHYAMA, N., AND KUBOTA, Y. Multispectral color imaging for dermatology: application in inflammatory and immunologic diseases. In *13th Color Imaging Conference* (Scottsdale, AZ, USA, 2005), pp. 52–58.

[87] YOON, G., PRAHL, S., AND WELCH, A. Accuracies of the diffusion approximation and its similarity relations for laser irradiated biological media. *Applied Optics 28*, 12 (1989), 2250–2255.

[88] YOON, G., WELCH, A., MOTAMEDI, M., AND VAN GEMERT, M. Development and application of three-dimensional light distribution model for laser irradiated tissue. *IEEE Journal of Quantum Electronics QE-23* (1987), 1721–1733.

[89] ZSCHEILE, F., AND COMAR, C. Influence of preparative procedure on the purity of chlorophyll components as shown by absorption spectra. *Botanical Gazette 102* (March 1941), 463–481.

[90] ZSCHEILE, F., JR., J. W., BEADLE, B., AND ROACH, J. The preparation and absorption spectra of five pure carotenoids pigments. *Plant Physiology 17*, 3 (July 1942), 331–346.

Annotated Slides

The full reference details for the papers mentioned during the course can be found in the bibliography section. The published papers that have been authored by the course presenter can be obtained from the following site:

$http://www.npsg.uwaterloo.ca/pubs/models.php$

Slide 1

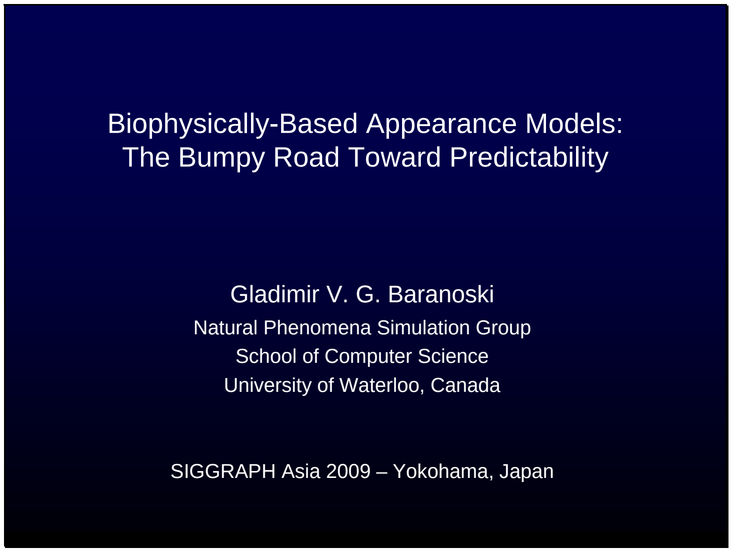

The main purpose of this course is to address practical issues involved in the development of biophysically-based light transport models used to simulate the appearance of natural materials within realistic image synthesis frameworks. Furthermore, since these models can also be employed in other scientific fields, it also aims to foster the cross-fertilization between computer graphics and these fields by highlighting common needs and complementary resources.

Slide 2

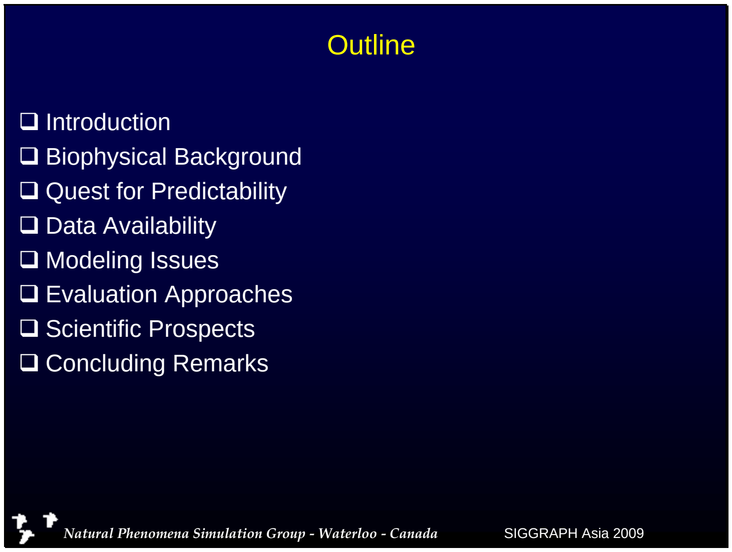

The course begins by providing a concise review of relevant biophysical background, followed by a discussion on the key concept of predictability. It continues by examining the specific constraints and pitfalls found in each of the key stages of the simulation framework, namely data collection, modeling and evaluation, and discussing alternatives to improve the fidelity of the entire process. Once a model is designed, implemented and evaluated through a sound methodology, its scope of applications can be expanded to address a wide range of scientific questions. For example, computer simulations are regularly being used by life science researchers to understand and predict material appearance changes prompted by mechanisms which cannot be fully studied using traditional experimental procedures. In line with this trend, the course closes with an examination of recent examples of computer graphics appearance models which can also be employed in such interdisciplinary research efforts.

Slide 3

One of the key components of the image synthesis pipeline corresponds to the modeling of how different materials reflect and transmit light so that they are assigned the appropriate appearance attributes such as color, glossiness and translucency [38]. Undeniably a significant progress has been achieved in this area. We have moved from ad hoc to physically-based models, and the impact on the realism of computer generated images was remarkable. Following this trend, computer graphics researchers started to look for computational solutions that would also lead to predictable simulations of materials' appearance. This course examines these modeling efforts from a scientific methodology point of view, i.e., judiciously looking at the different stages of the simulation framework to point out practical and scientific issues usually overlooked by the existing simulation approaches.

Slide 4

More specifically, this course addresses the modeling of light interactions with natural materials, organic and inorganic. Common examples of these materials include plants and human tissues (e.g., skin, hair and iris).

Slide 5

Among the inorganic materials, we can include water as well as particulate materials (e.g., sand).

Slide 6

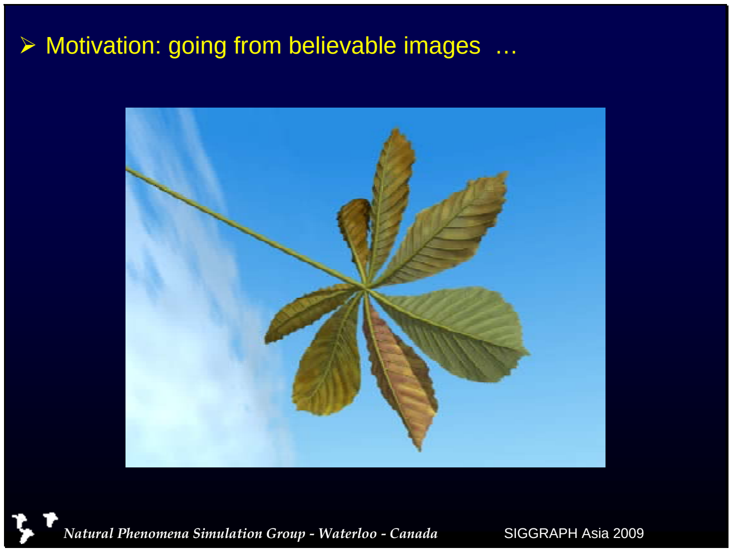

The motivation for this course involves the design of models that can be used not only to generate believable images depicting these materials [35], but also to provide predictable results.

Slide 7

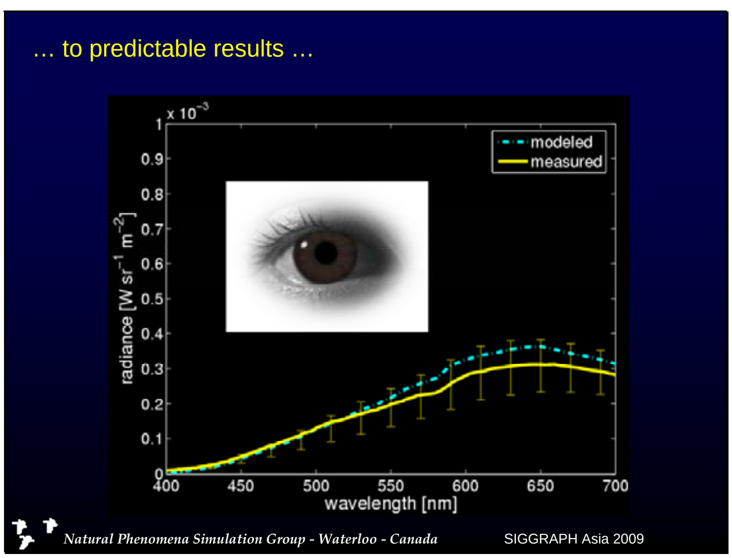

The verification of predictability can be performed through comparisons of modeled results with experimentally measured data [30].

Slide 8

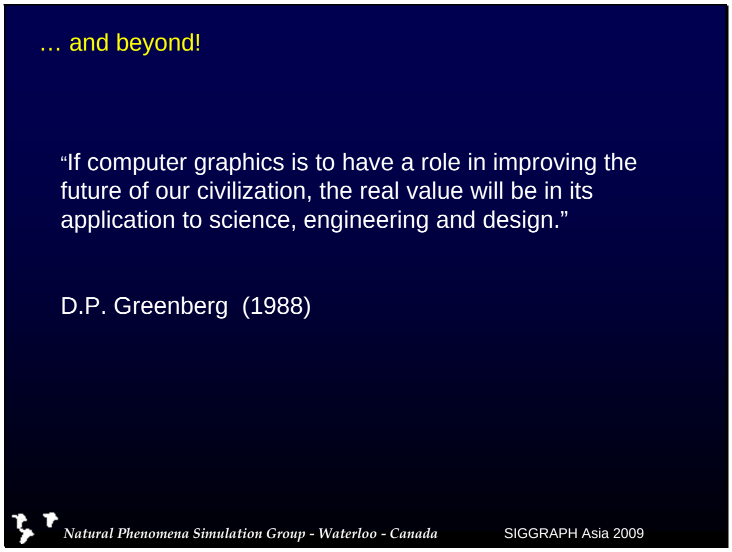

Ultimately, these predictive models can also be used in a wide range of scientific applications such as the remote sensing of natural resources [41] and noninvasive diagnosis of medical conditions [74].

Slide 9

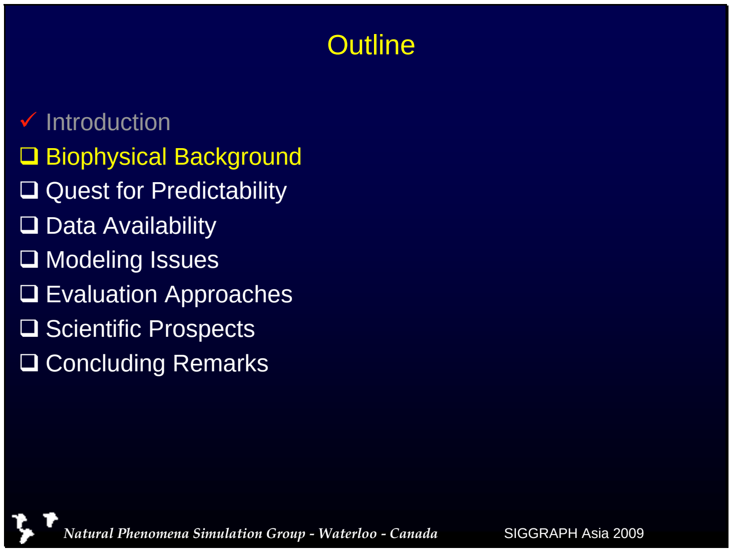

.

Slide 10

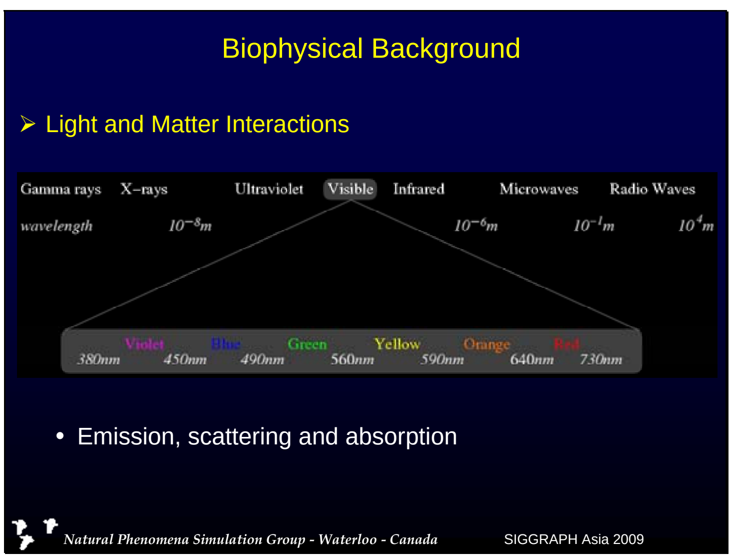

Light is a form of energy, which includes not only the visible light, but also other forms of electromagnetic radiation such as microwaves and X-rays. The problem of determining the appearance of a material involves the simulation of light interactions with matter, which, in turn, can be classified into three main processes: emission, scattering and absorption.

Slide 11

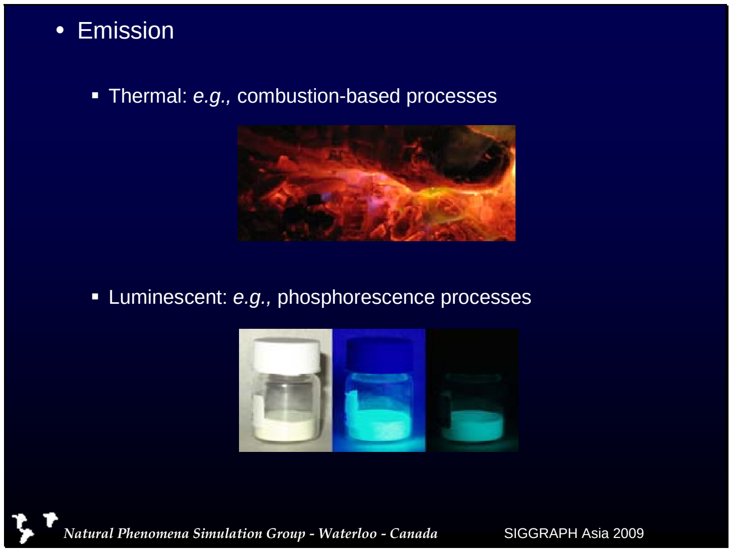

Man made and natural light sources emit light with characteristic spectral distributions, which depend on the nature of the emission process. The processes of light emission can be divided into two types: thermal and luminescent [14]. Thermal emissions are due to the material radiating excess heat energy in the form of light. For these materials, called thermal radiators, the amount of light emitted is primarily dependent on the nature of the material and its temperature. Luminescent emissions are due to energy arriving from elsewhere, which is stored in the material and emitted (after a short period of time) as photons. The incident energy, primarily due to factors other than temperature, causes the excitation of electrons of the material. These electrons in the outer and incomplete inner shells move to a higher energy state within the atom. When an electron returns to the ground state a photon is emitted. The wavelength of the emitted photon will depend on the atomic structure of the material and the magnitude of the incoming energy.

Slide 12

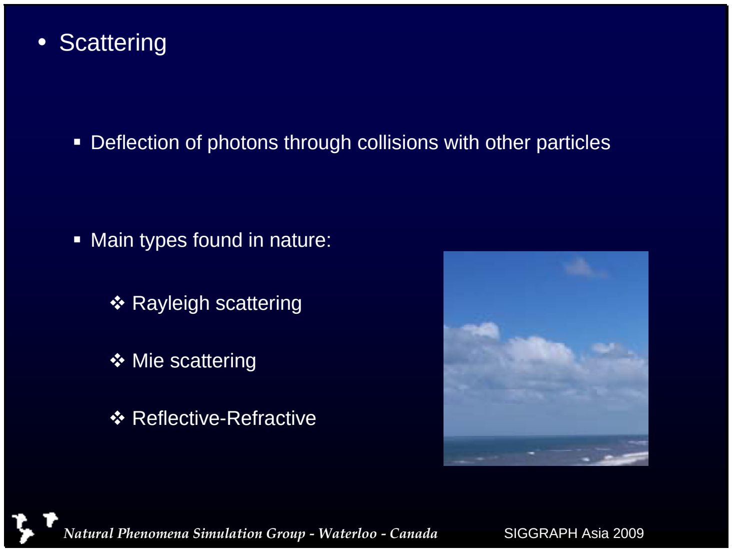

The three main types of scattering occurring in Nature are the following: Mie, Rayleigh and reflective-refractive scattering. Mie, or aerosol, scattering occurs when the wavelength of the radiation is comparable to the size of the molecules, or particles, through which is passing. Rayleigh, or molecular, scattering occurs when the wavelength of the radiation is somewhat larger than the molecules, or particles, through which it is passing. It is proportional to the fourth power of the frequency, and hence the shorter wavelengths are preferentially attenuated. As the particles get larger, scattering tends to be more uniform across the spectrum [67]. Reflective-refractive accounts for most of the internal scattering occurring in organic tissues such as plant leaves and human skin. It is mainly caused by the arrangement of tissues, and the refractive differences, which, for the most part, are associated with air-cell wall interfaces with respect to cells whose dimensions are quite large compared with the wavelength of light. Due to its dependency on the refractive differences, the variations across the spectrum are directly associated with the wavelength dependency of the refractive indices of the materials.

Slide 13

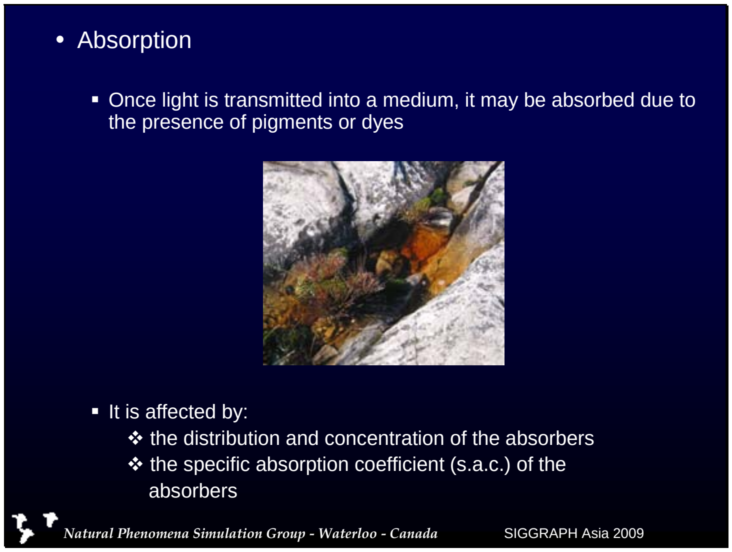

Once light is transmitted into a medium, it may be absorbed in a dielectric. This will happen if there are absorptive elements, such as pigments and dyes, inside the medium. Pigments are materials that exhibit selective scattering and selective absorption, while dyes exhibit selective absorption and some luminescence produced due to excitation [24]. The spectral distribution of light due to the absorption process depends on the distribution, concentration and absorption spectra of the absorptive elements, which, in turn, is determined by the type of chromophore, or molecular functional group, affecting the capture of photons.

Slide 14

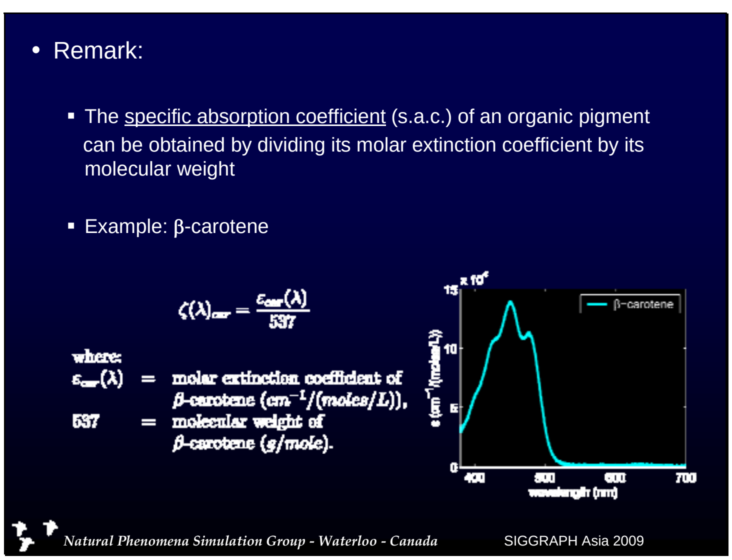

Slide 15

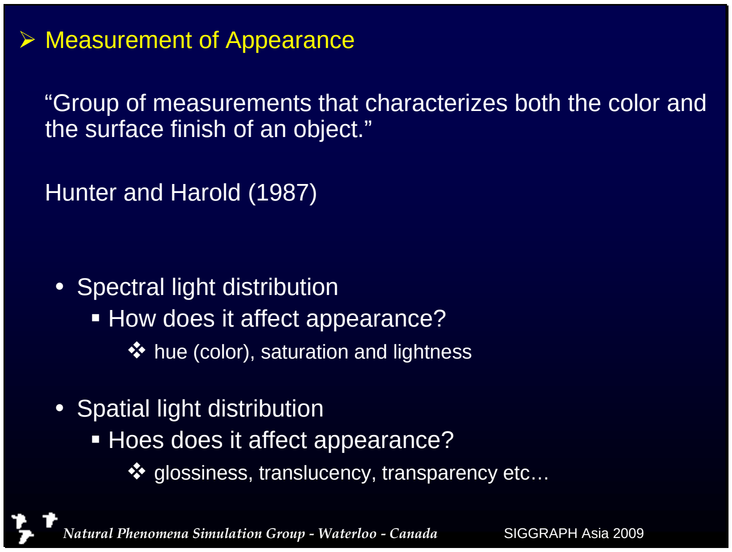

The group of measurements necessary to characterize both the color and surface finish of a material is called its measurement of appearance [38]. These measurements involve the spectral and the spatial energy distribution of propagated light. The variations in the spectral distribution of the propagated light affect appearance characteristics such as hue, lightness and saturation. The changes in the spatial distribution of the propagated light affect appearance characteristics such as glossiness, transparency and translucency.

Slide 16

Slide 17

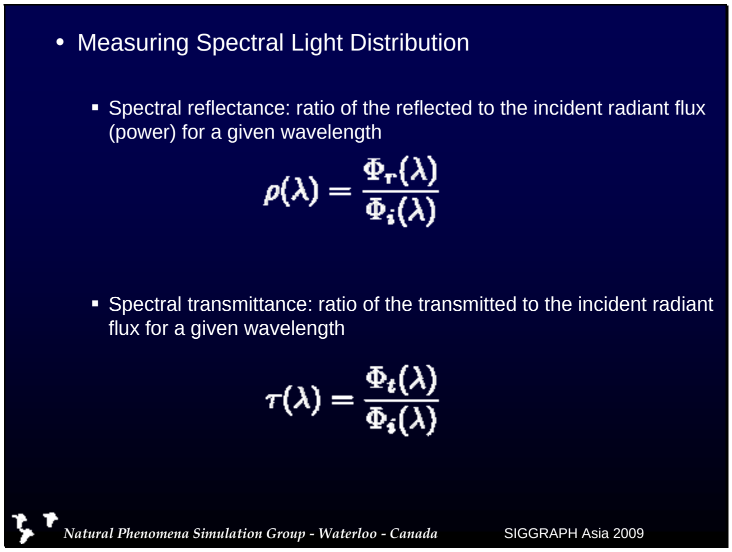

There are nine different representations of reflectance and transmittance. These representations depend on the incident and propagated (collected) light geometries, which are designated as directional, conical and hemispherical [58].

Slide 18

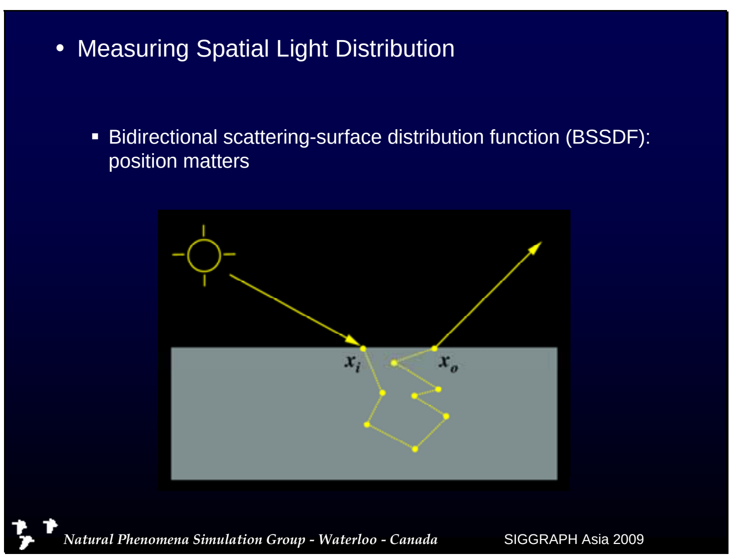

The spatial patterns of light distribution are represented by the bidirectional scattering-surface distribution function (BSSDF), or its components: the bidirectional scattering-surface reflectance distribution function (BSSRDF) and its counterpart the bidirectional scattering-surface transmittance distribution function (BSSTDF) [58].

Slide 19

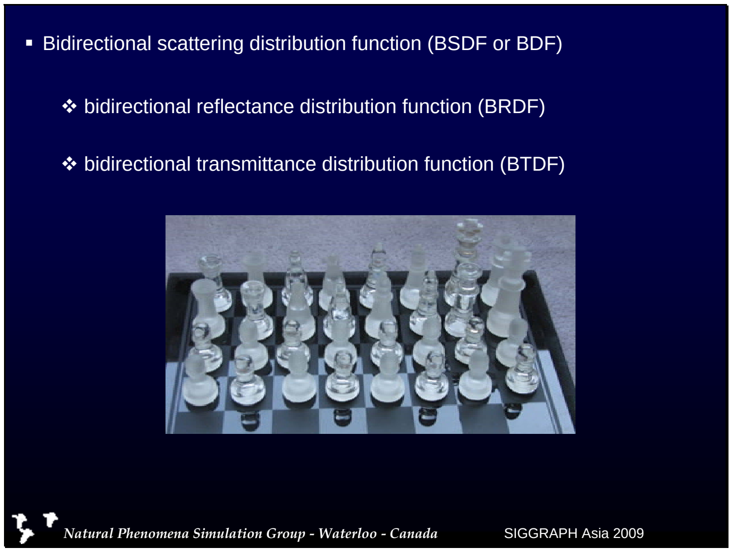

The BSSDF is considered to be a difficult function to measure, store and compute due to its dependency on four parameters: the incidence and outgoing directions, the wavelength and the position on the surface. For this reason, sometimes it is more practical to make simplifying assumptions about the material in order to obtain a more tractable function, and still obtain a useful degree of approximation for the cases of interest. For example, if one assumes that a given material's scattering properties are uniform, the dependence on the location of the point of observation (reflection) can be omitted [58]. In this case, one can work with a simpler function, namely the bidirectional scattering distribution function (BSDF, or simply BDF), which can also be decomposed into two components: the bidirectional reflectance distribution function (BRDF) and the bidirectional transmittance distribution function (BTDF).

Slide 20

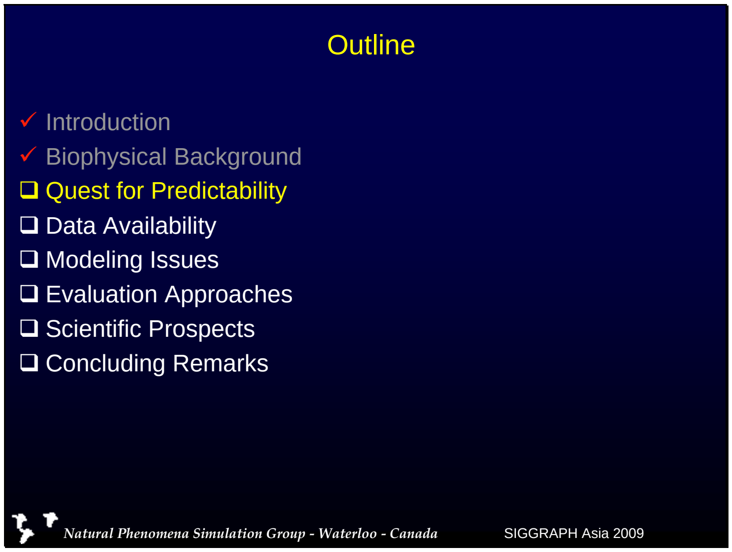

Believable images may result from biophysically-inspired simulations. They are usually aesthetically pleasing and realistic. Predictable images, on the other hand, result from biophysically-based simulations whose accuracy is evaluated through comparisons with experimental data. Predictive simulations, however, do not guarantee the generation of images with a higher degree of realism, which may be affected by errors introduced in other components of an image synthesis framework.

Slide 21

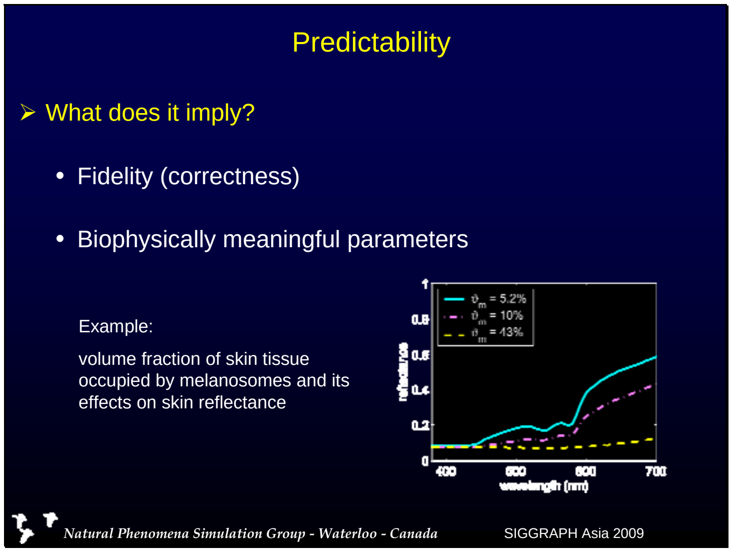

In 1997, Greenberg et al. [30] discussed the importance of predictive simulations and its broader range of application beyond picture making. This panel also pointed out that in order to be predictive, one must prove that the simulations are correct, and fidelity is the key in this context. But, what is fidelity?

“The degree to which a model or simulation reproduces the state and behavior of a real world object or the perception of a real world object, feature, condition or chosen standard in a measurable or perceivable manner; a measure of realism of a model or simulation; faithfulness [31].”

The biosynthesis of melanin takes place in membranous organells, called melanosomes, found in the long filaments of melanocyte cells. In healthy skin, these cells are located in the epidermis, more specifically in the stratum basale. The melanin absorption level depends on how many melanosomes per unit volume are in the epidermis. Typically, the volume fraction of the epidermis occupied by melanosomes varies from 1.3% (lightly pigmented specimens) to 43% (darkly pigmented specimens) [43]. The skin of individuals with a genetic predisposition to a lower concentration of melanosomes tend to have a spectral signature characterized by higher reflectance values which vary considerably in the region between 500nm to 600nm. The lower amount of melanin in this case makes the effects of light absorption by oxyhemoglobin (a natural pigment found in human blood) to become more prominent. Hence, the variations in the absorption spectrum of oxyhemoglobin in this region result in the characteristic ``W" shape observed in the spectral signature of moderately or lightly pigmented skin specimens. This phenomenon can also be observed in the spectral curves (above) obtained using the BIOSPEC model [48].

Slide 22

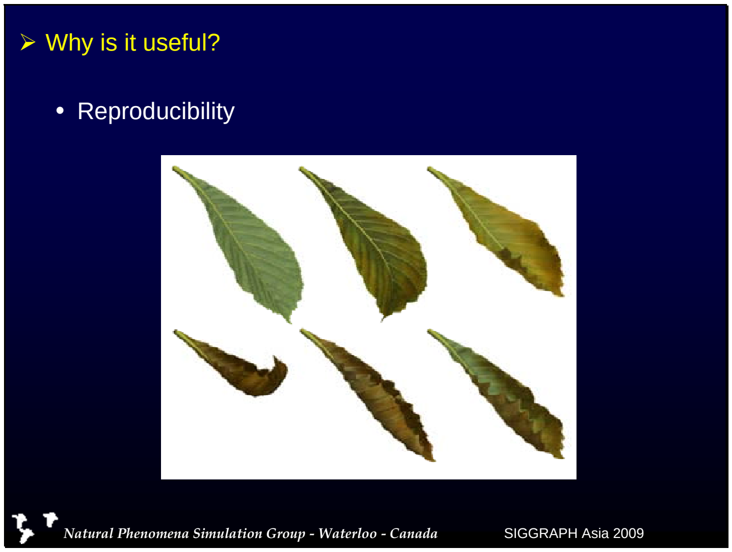

One may ask what practical benefits can arise from investing more time and resources to design and implement predictive simulations. First, they can contribute to make the image generation process more automatic since they are controlled by biophysically meaningful parameters, which facilitates the reproduction of their results. Second, they have a wider range of scientific and medical applications.

Slide 23

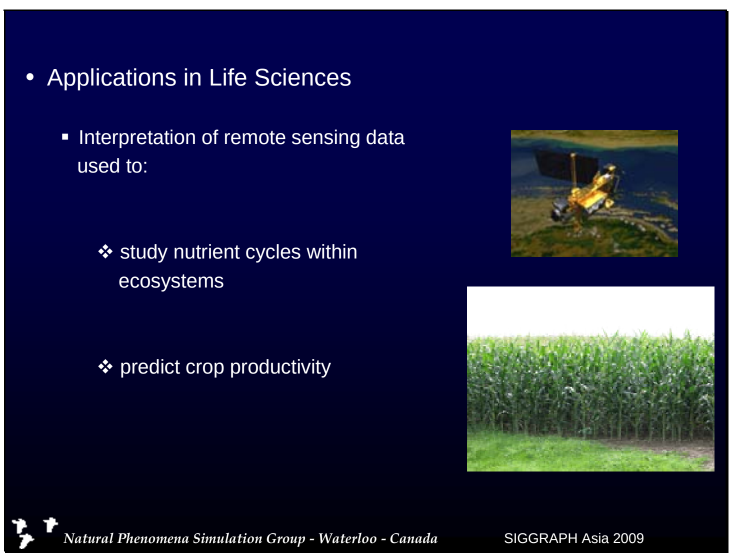

Slide 24

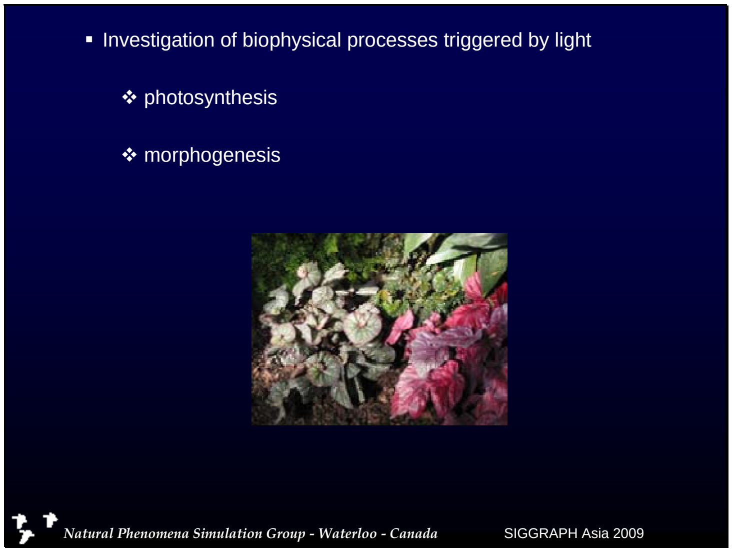

Slide 25

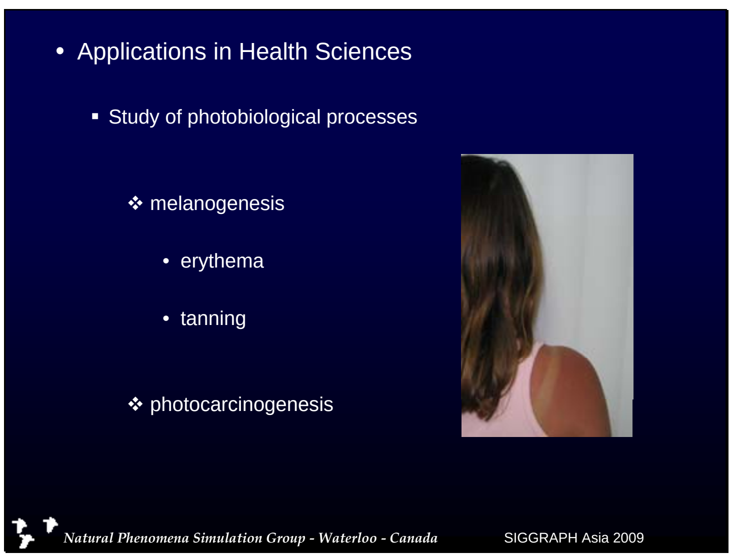

Ultraviolet radiation, notably UV-B (ranging from 280nm to 315nm), penetrates in skin layers, and it may increase melanogenesis (biosynthesis of melanin) after a certain period (6-8 hours) that follows an erythema reaction (a reddening around the stimulus site due to a dilation of the blood vessels, which increases the volume fraction of blood in the dermis layers [59]). It is responsible for the development of tan. Overexposure to ultraviolet radiation can, however, induce photocarcinogenesis, i.e., a series of biochemical events that ultimately lead to the formation of skin cancer (e.g., carcinomas and melanomas) [25,60].

Slide 26

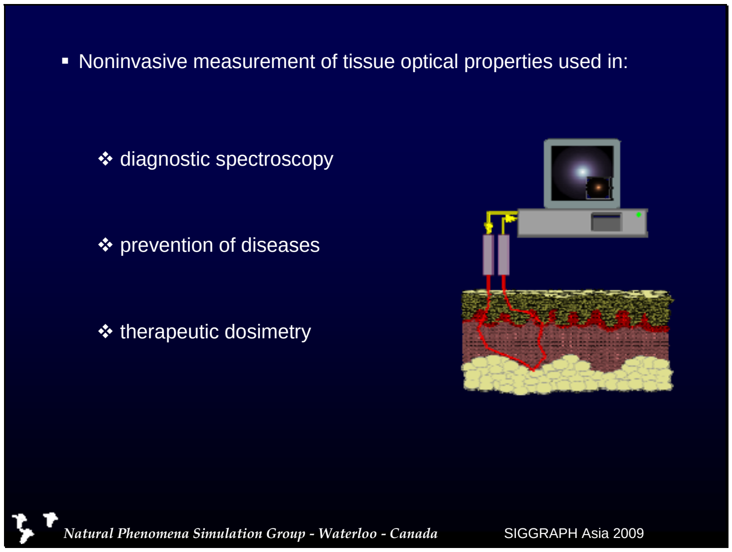

The models of light interaction with human skin developed by the scientific community are usually designed to support noninvasive measurement of tissue optical properties to be used in the diagnosis [72,86], prevention [61] and treatment of skin diseases [18,69]. It is worth noting that a substantial portion of the modeling work done in these fields is either laser-based or aimed at wavelengths outside the visible region of the light spectrum (ultraviolet and infrared domains). Some medical applications, such as phototherapy for the treatment of skin inflammatory diseases or photodynamic therapy for the treatment of skin cancer, require *in vivo* light dosimetry, i.e., the measurement of radiant energy fluence rate, given in terms of irradiance (radiance integrated over all directions), and fluence (the time integral of the fluence rate) [69].

Slide 27

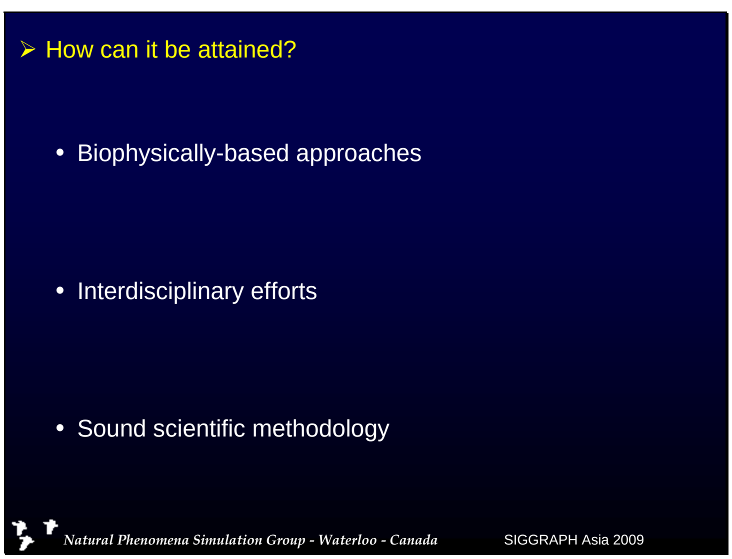

Slide 28

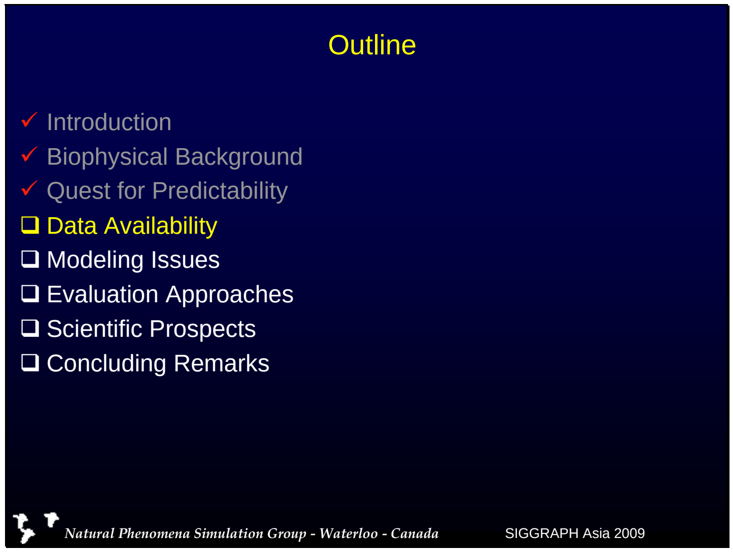

Slide 29

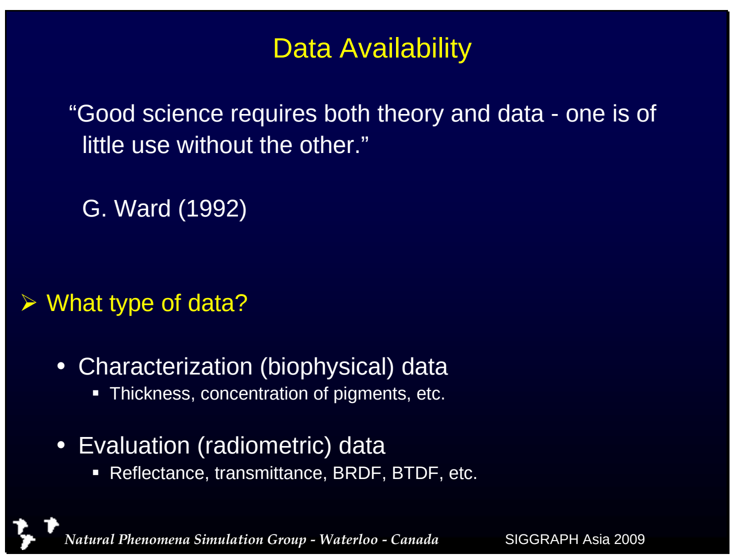

Slide 30

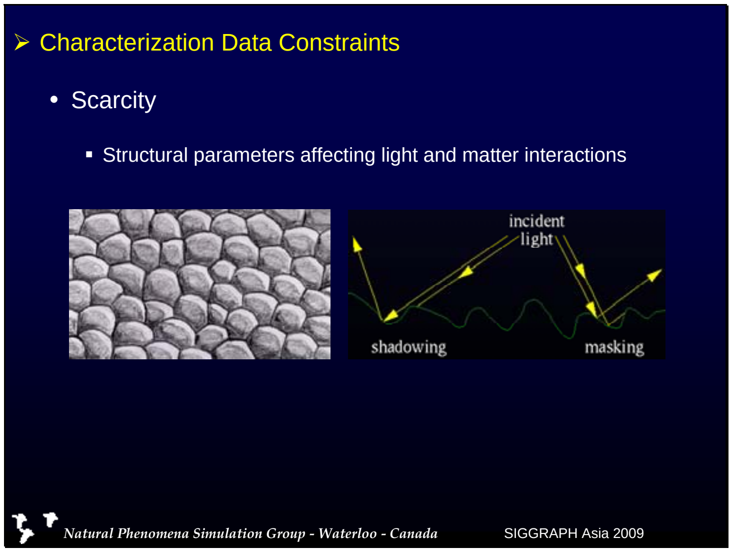

Slide 31

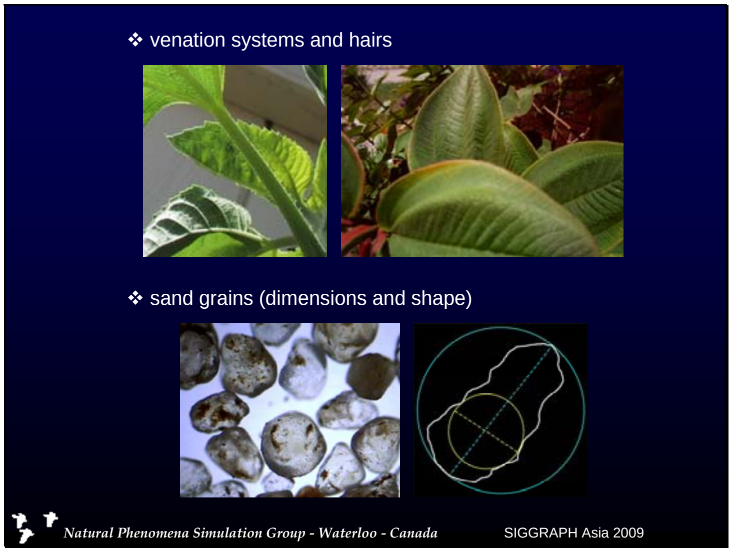

The shape of the grain is described by two quantities; sphericity and roundness. In our modeling of sand appearance attributes [47], we used the sphericity measure proposed by Riley [64], which corresponds to the square root of the ratio of the diameter of the inscribed circle by the circumscribed circle.

Slide 32

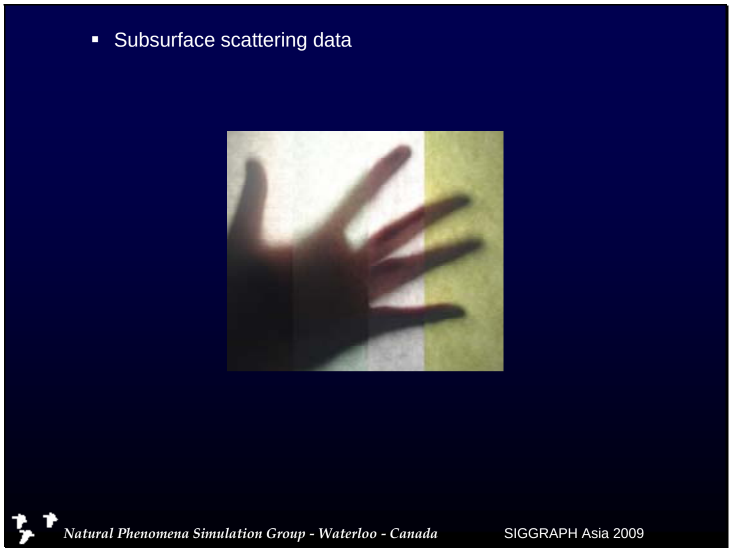

Slide 33

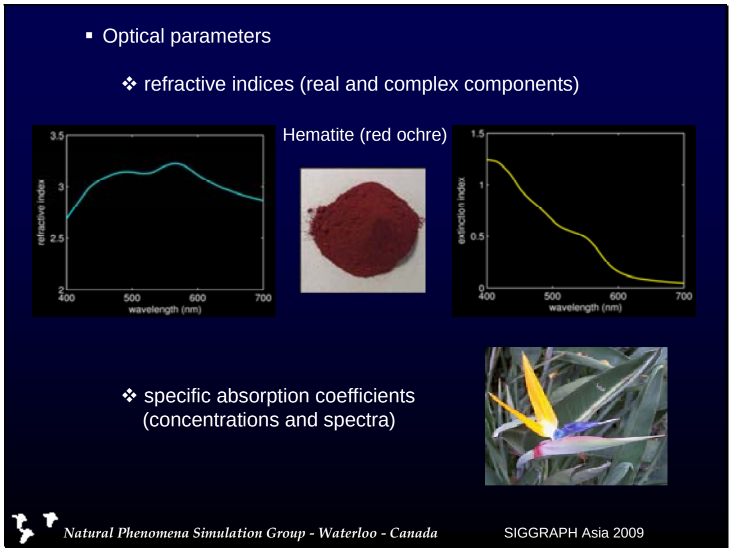

There are many conflicting sources of refractive index data. For example, in our modeling of sand appearance attributes [47], we used hematite data extracted from plots by Sokolik and Toon [68] because it was the only source of data we found that covered the entire visible range, provided complex refractive index data directly, and was not acquired using a method known to have problems [46].

Slide 34

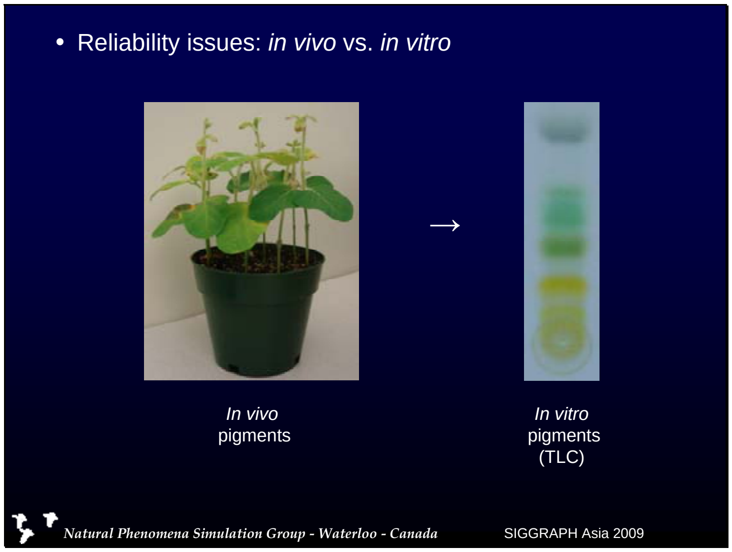

Thin-layer chromatography (TLC) is a procedure used to separate the chemical components of a solution [21].

Slide 35

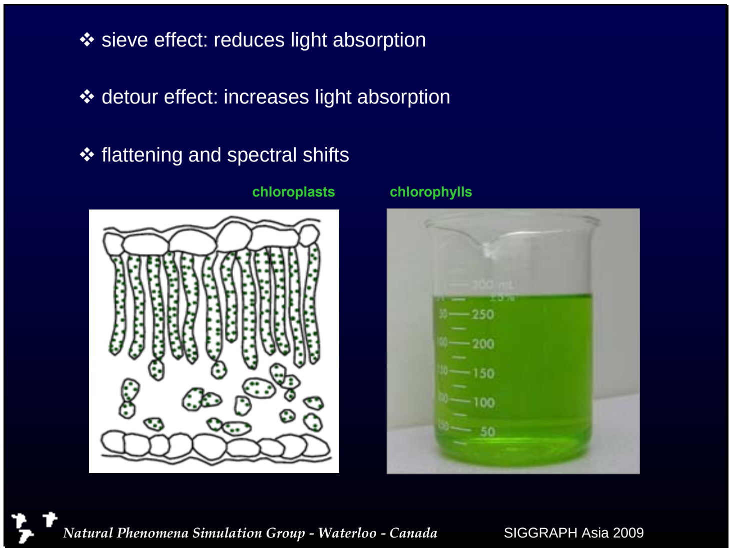

Sieve effects (light that passes through tissues without encountering an absorber) and detour effects (light that is scattered and has an increased path length) affect *in vivo* light absorption [3]. The organic solvents used to prepare pigment extracts can alter pigment-protein bonds, which may result in shifts and flattening of their in absorption spectrum measured under *in vitro* conditions [22].

Slide 36

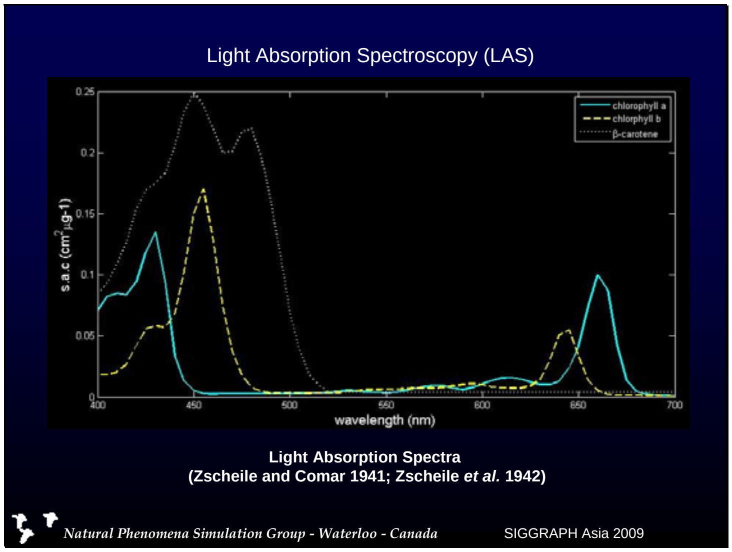

Slide 37

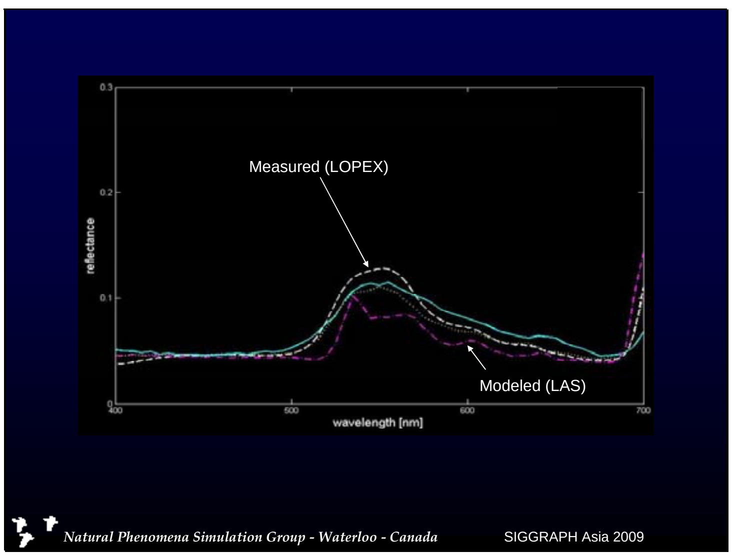

The Leaf Optical Properties Experiment (LOPEX) data set [36] contains biophysical and spectral data routinely used in the validation of models of light interaction with plants. The modeled curves were generated using the ABM-B (algorithmic BDF (bidirectional scattering distribution function) model for bifacial leaves) [1,3].

Slide 38

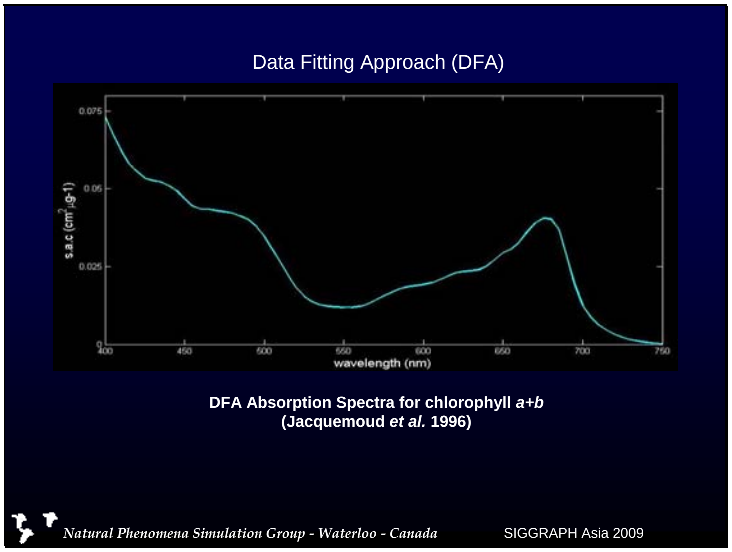

Slide 39

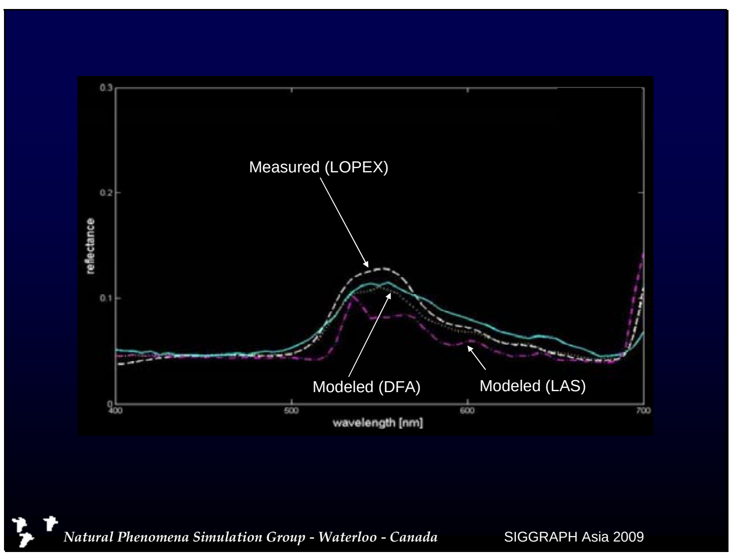

Slide 40

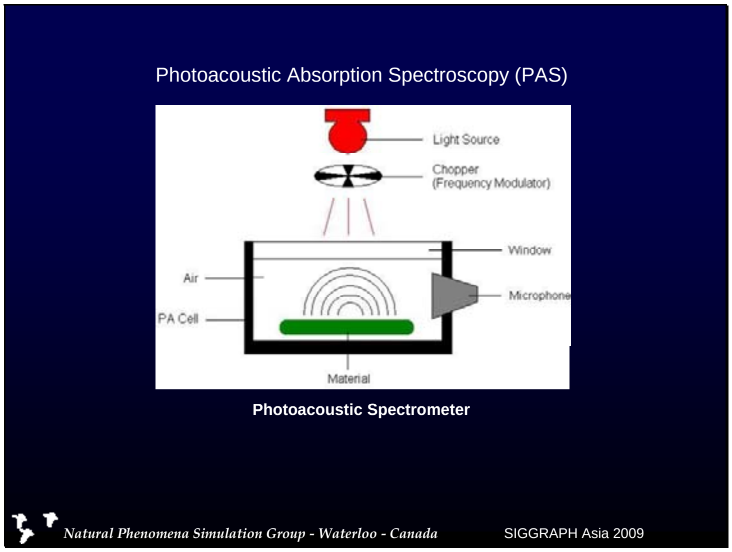

“PAS uses pulsed light to illuminate a sample in an enclosed gas-filled cell that is referred to as a photoacoustic cell. The incident light is absorbed, which causes the sample to enter into an excited state. Deexcitation of the sample can take place in a number of different ways including the reradiation of the absorbed energy as thermal energy or heat. When the sample radiates heat, it also raises the temperature of the surrounding gas and, correspondingly, the pressure inside of the photoacoustic cell. The pulsed nature of the incident light causes the pressure to change in a similar manner, generating waves that can be picked up with a detector, such as a microphone. Plotting the relative signal strength generated by the sample at different wavelengths of incident light produces a photoacoustic absorption spectrum, which qualitatively resembles that of an absorption spectrum. PAS has many advantages over other forms of spectroscopy including the ability to obtain the optical and thermal properties of highly scattering solid and semisolid materials such as powders, gels, suspensions, and tissues [22].”

Slide 41

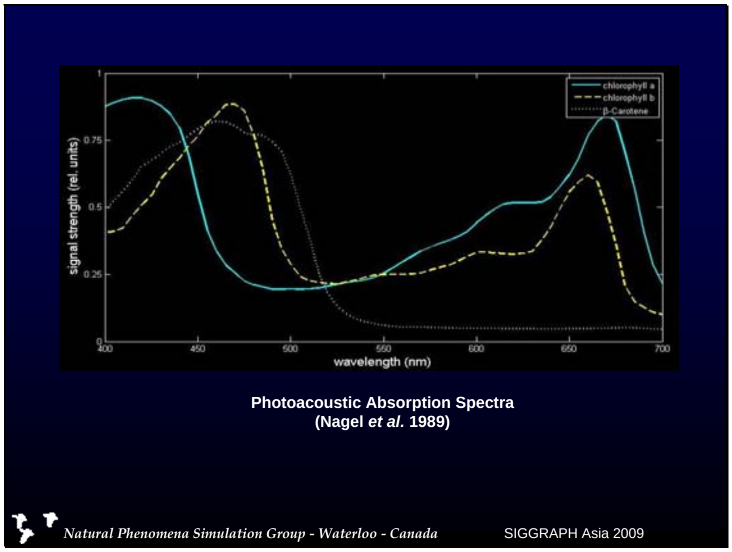

Slide 42

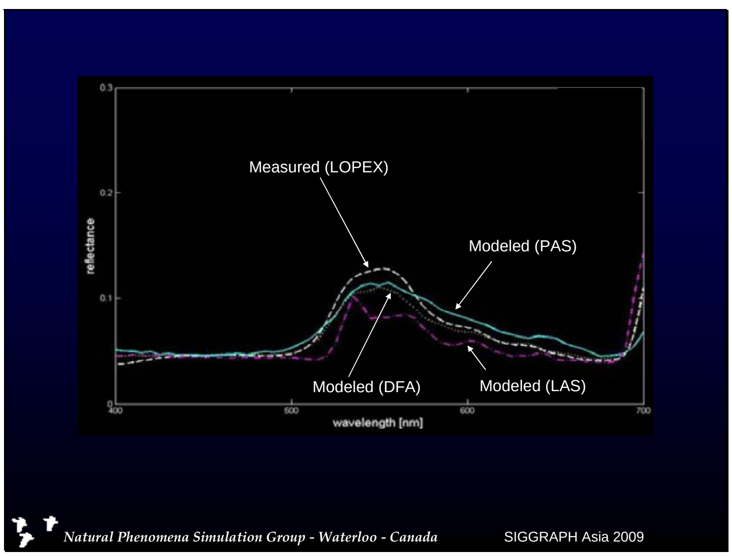

Slide 43

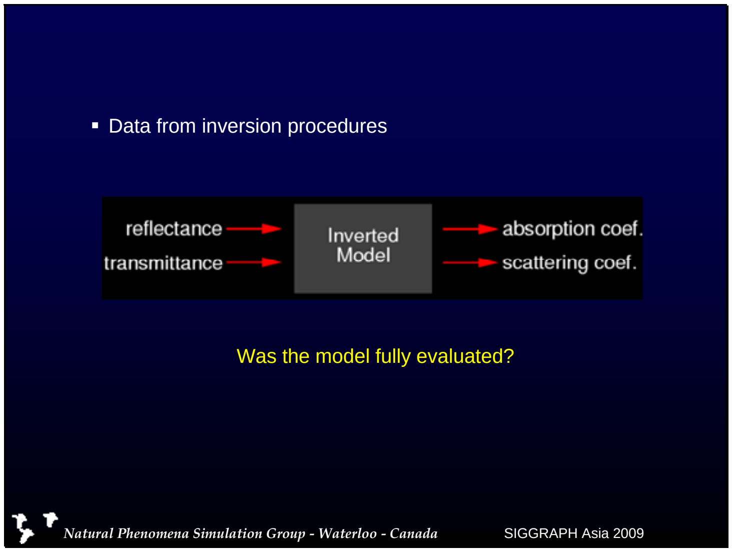

An inversion procedure is a way to derive biochemical and optical properties from *in situ* and noninvasive measurements. These measurements, which often correspond to spectral reflectance and transmittance, are usually obtained by placing a sensor against or at some distance from the tissue. The term ``inversion'' in this context implies a reversal of the actual process of calculating reflection and transmission, i.e., using reflectance and transmittance values as input, one can determine absorption and scattering properties of the tissues (given in terms of volumetric absorption and scattering coefficients).

Slide 44

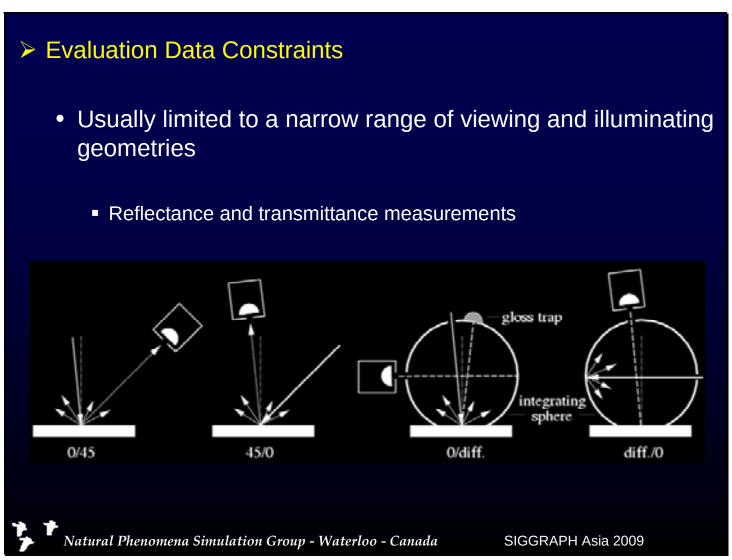

Slide 45

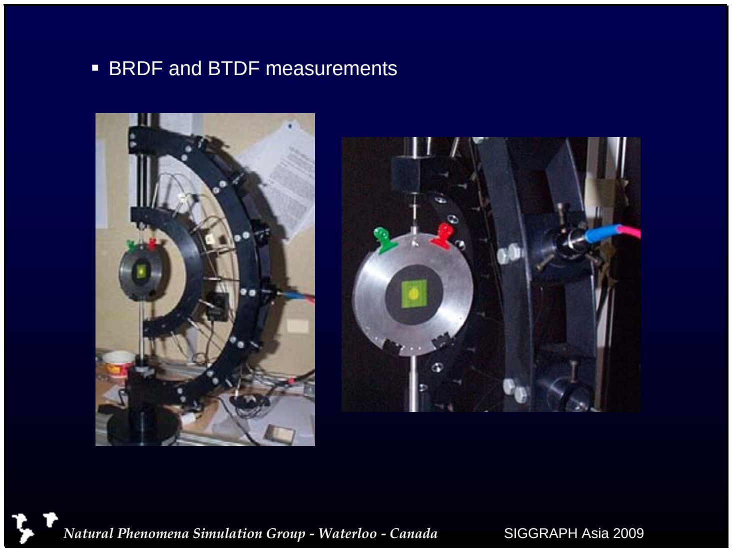

Slide 46

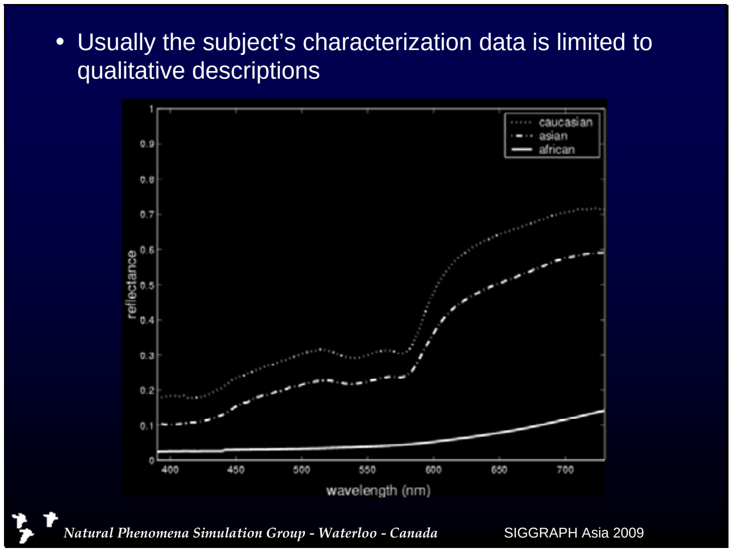

Data source: North Carolina State University (NCSU) spectra database [80].

Slide 47

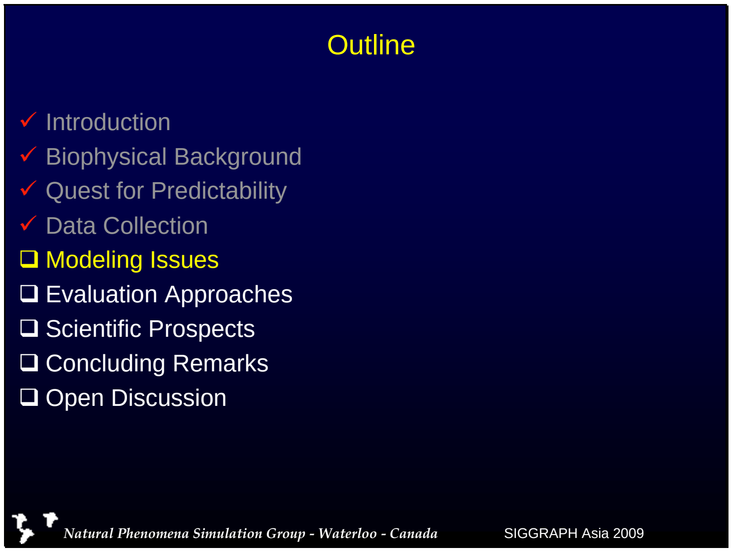

Slide 48

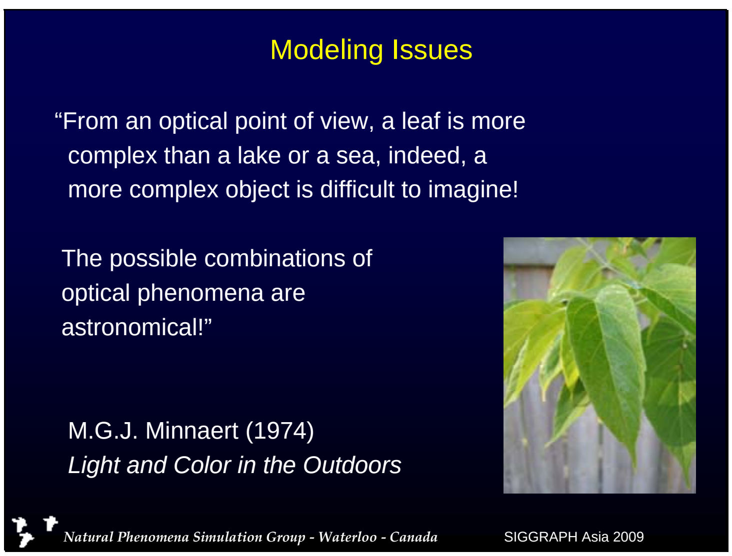

Slide 49

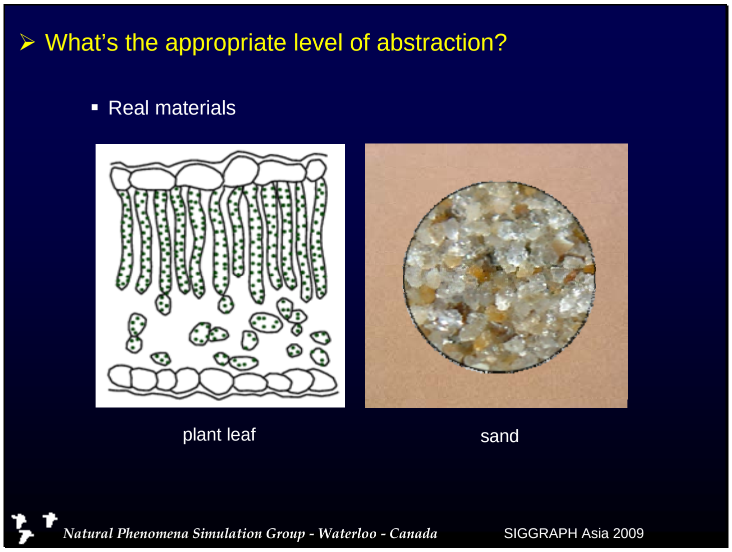

Slide 50

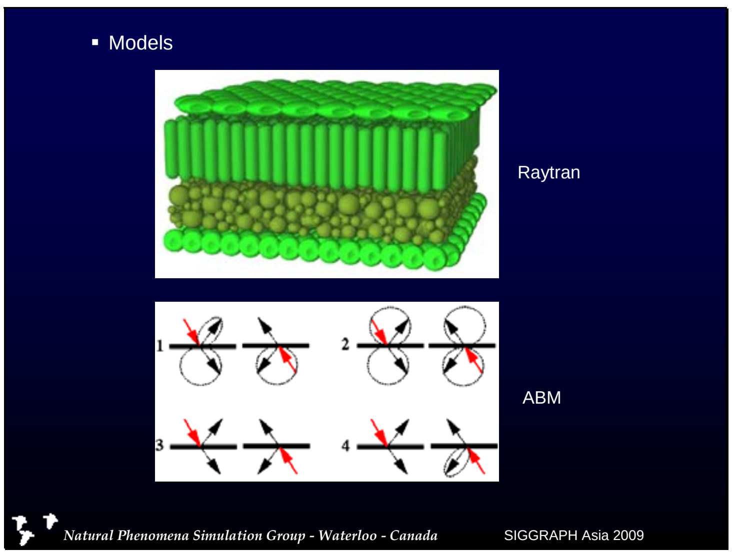

There are models that simulate light transport by geometrically representing a material's internal structures (e.g., Raytran model [27]). At the other end, there are models that use the intuitive concept of layers in which the properties of the material's internal structures are globally described through mathematical expressions, i.e., using pre-computed functions to represent the bulk scattering of light within a given layer (e.g., ABM model [9]).

Slide 51

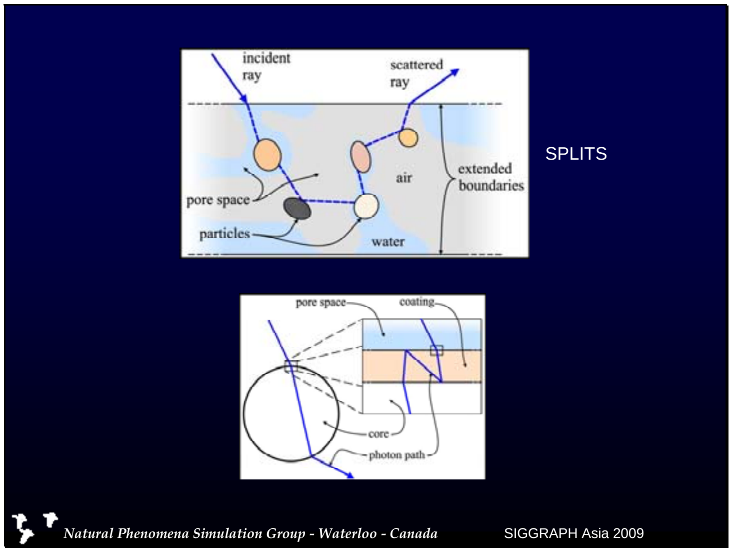

Alternatively, it is also possible to compute directional changes on the fly taking into account the geometrical characteristics of the material's individual structures without explicitly storing them (e.g., the SPLITS model [47]).

Slide 52

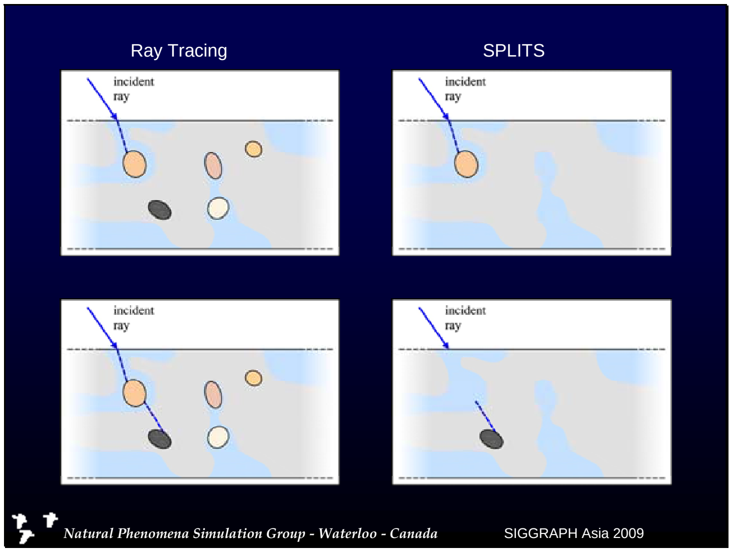

Slide 53

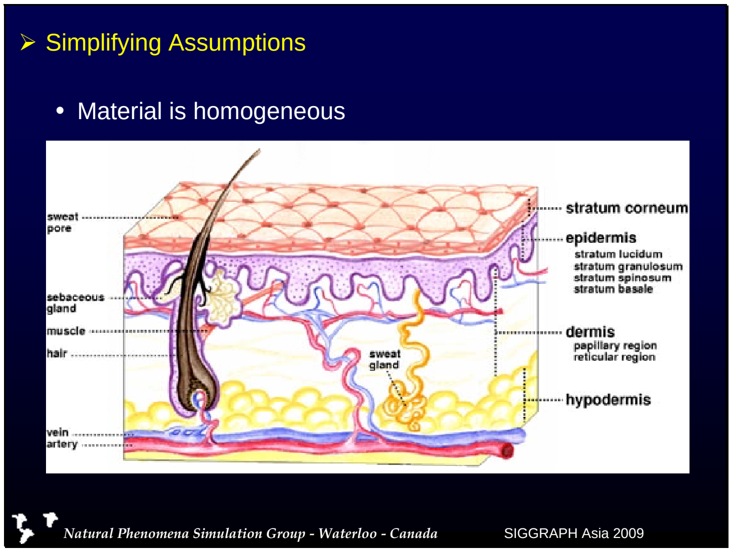

Clearly, it may not be practical to consider all layers and sublayers that form a material due to either lack of data or computational complexity. For example, most of the skin descriptions employed in studies of skin optics depict three main layers, namely stratum corneum, epidermis and dermis, which are usually assumed to be homogeneous.

The first and outermost section of human skin is the stratum corneum, which is a stratified structure approximately 0.01-0.02mm thick [48]. There are skin structural models, however, that consider it part of the epidermis [74]. The stratum corneum   is composed mainly of dead cells, called corneocytes, embedded in a particular lipid matrix [71].

The epidermis is a 0.027-0.15mm thick structure 48] composed of four main layers (stratum basale, stratum spinosum, stratum granulosum and stratum lucidum).

The dermis is a 0.6-3mm thick structure [48]. It can be divided into two regions: the papillary dermis and the reticular dermis. These regions are primarily composed of dense, irregular connective tissue with nerves and blood vessels (smaller ones in the papillary, and larger ones in the reticular dermis).

The hypodermis is an adipose tissue, which is usually not considered part of the skin. Its size varies considerably throughout the body. It can be up to 3cm thick in the abdomen and absent in the eye lids. The hypodermis presents significant deposits of white fat, whose cells are grouped together forming clusters.

Slide 54

Anisotropy is observed when the material is rotated around its normal, while the light and the viewer directions remain unchanged, and the light intensity reflected to the viewer varies. Most natural materials are anisotropic, i.e., their reflection profile depends on both the polar and the azimuthal angles measured from the material's normal, and used to define the direction of incidence of the incoming light. For example, leaves with a parallel venation system (specimen on the left) reflect light more diffusively in a plane perpendicular to their veins [10]. For practical reasons (e.g., lack of supporting data), however, natural materials are often assumed to be isotropic, i.e., the dependence of their reflection profile on the azimuthal angle of light incidence is often omitted in light transport simulations leading to the modeling of their appearance.

Slide 55

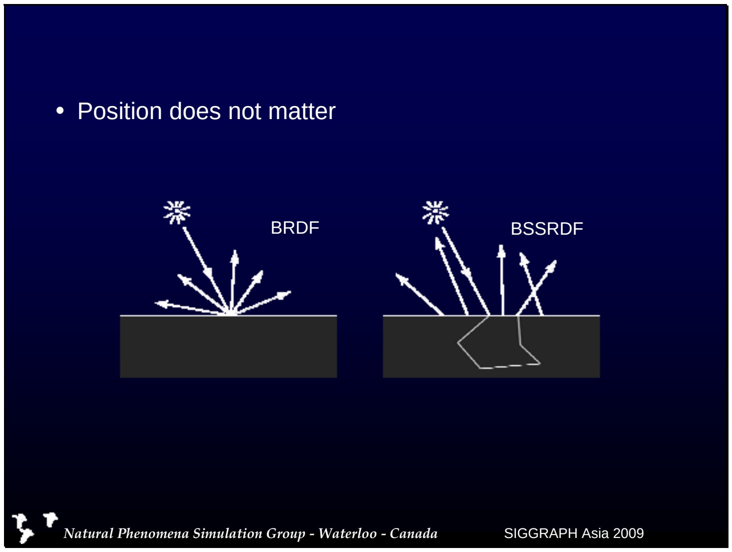

Slide 56

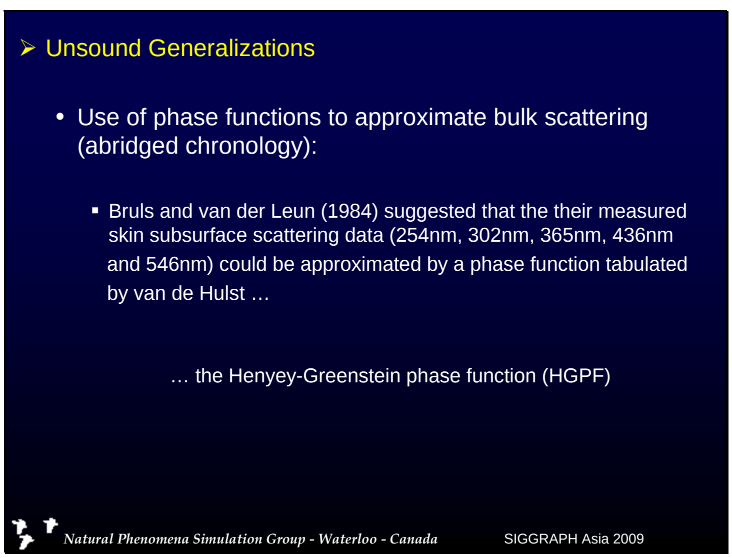

When light hits a particle with an index of refraction different from that of its environment, the light is scattered. A phase function describes the amount of light scattered from the direction of incidence to the direction of scattering [75,76,77], i.e., it represents a single scattering event. The HGPF was proposed by Henyey and Greenstein [33] to approximate Mie scattering in their study of diffuse radiation in galaxies.

Slide 57

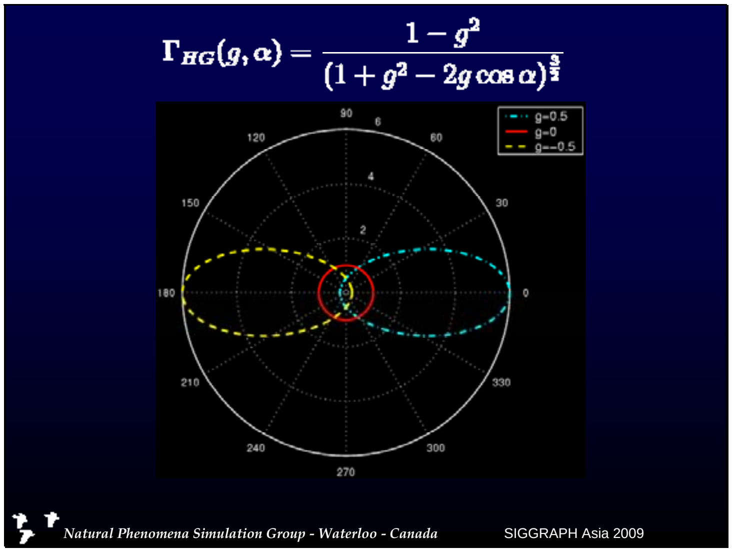

The average cosine of the phase function, or asymmetry factor *g*, is used to describe the degree of asymmetry of the phase function. It is often “anisotropy factor” which may result in a misleading association with the macroscopic anisotropic behavior of a given material.

Slide 58

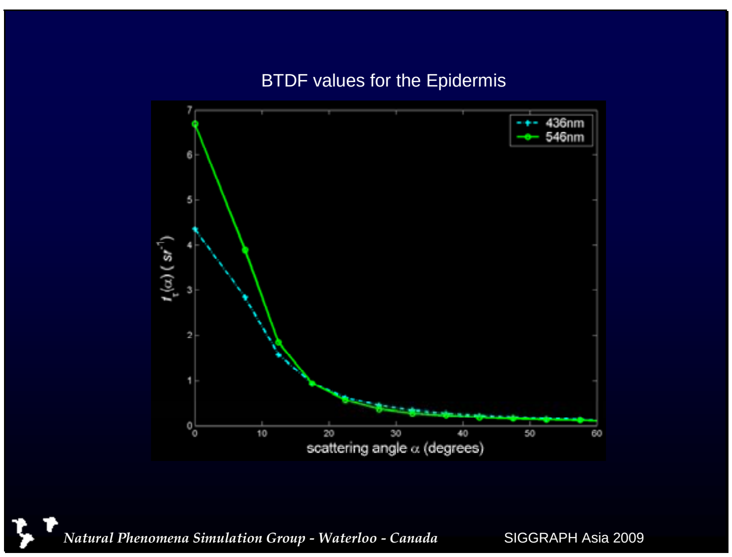

These curves were computed by Baranoski et al. [7] using scattering data measured by Bruls and van der Leun [13].

Slide 59

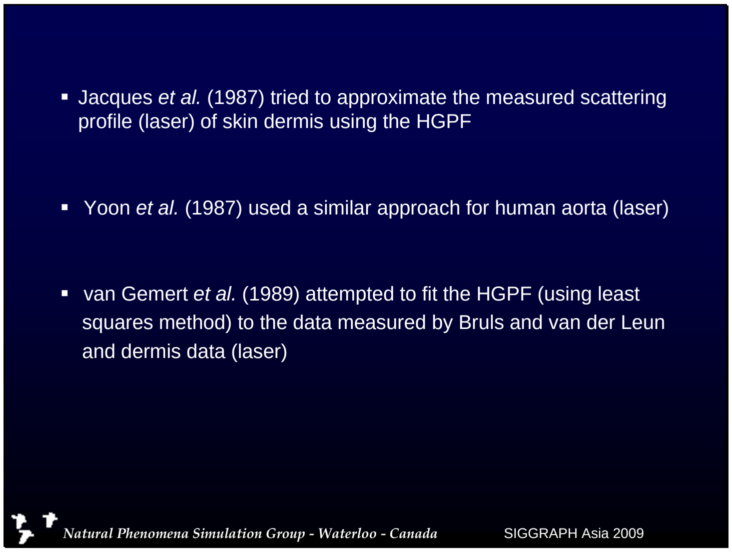

Jacques et al. [44] appropriately stated that ``the use of the HG function to specify radiant intensity for thicker samples is only descriptive, and should be distinguished from the customary use of the HG function to described single particle phase function".

Slide 60

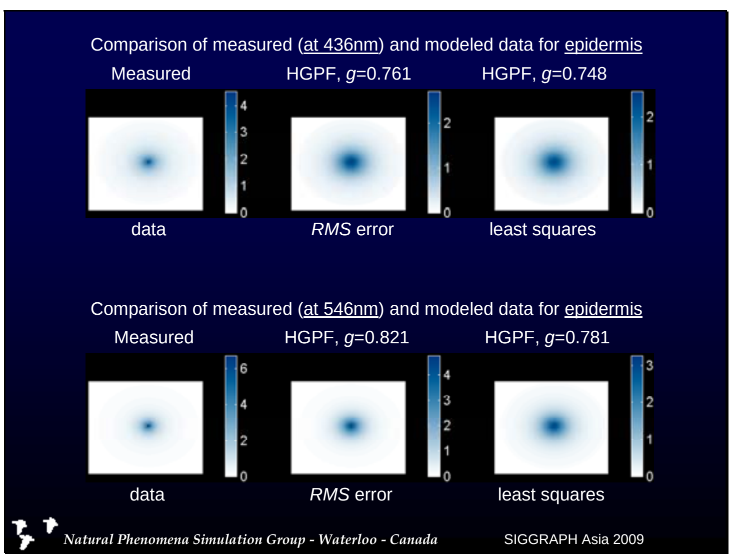

Slide 61

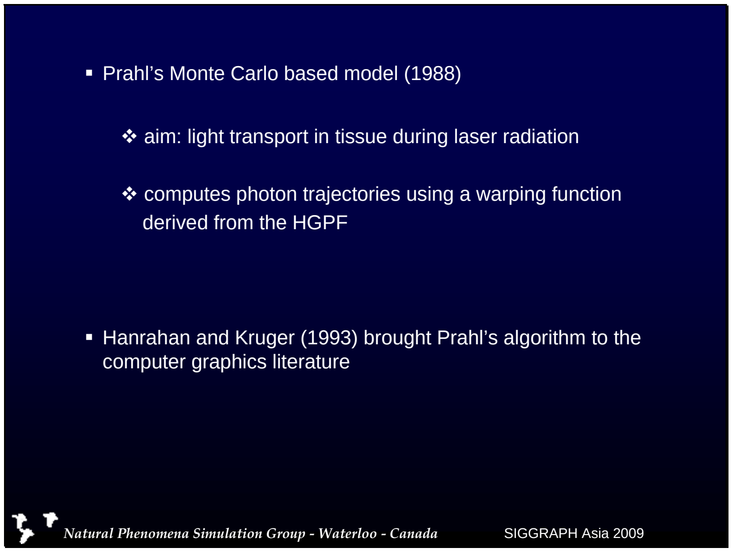

Slide 62

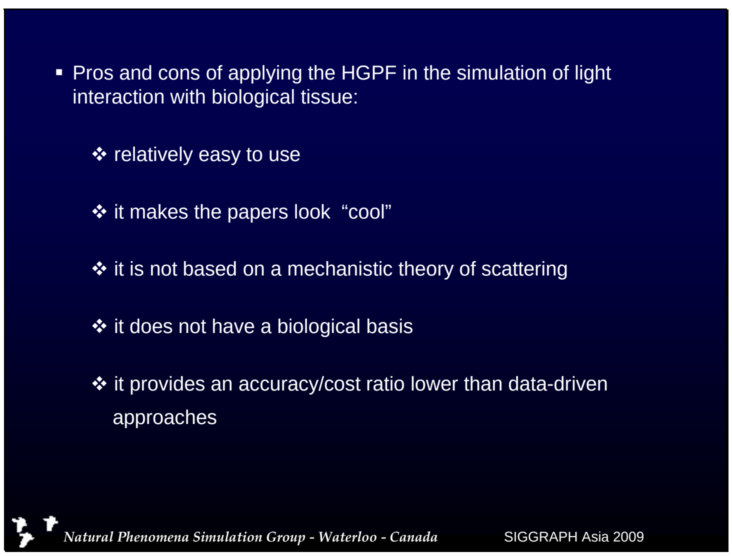

We remark that the HGPF is neither based on the mechanistic theory of scattering [44], nor was it originally devised to approximate the bulk scattering of complex materials [6,7,15,51]. Although its use may be justifiable in the absence of measured scattering data or more accurate approximations, when such data is available a more effective option is to use the data directly (e.g., through simple table look-ups [6,7]).

Slide 63

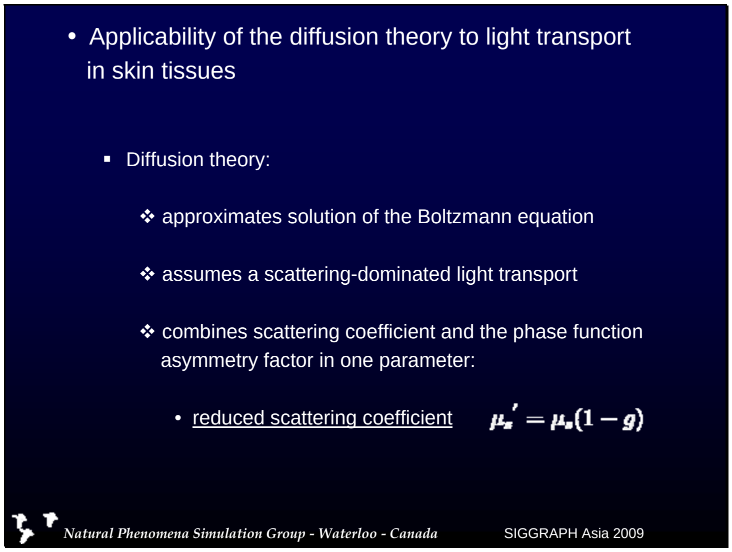

Photon propagation in optically turbid media, such as skin tissues, can be described by the time and energy independent equation of radiative transport known as the Boltzmann photon transport equation [34,40]. This equation requires the optical properties of the medium to be expressed in terms of scattering coefficient, absorption coefficient and phase function. Diffusion theory can be seen as an approximate solution of this equation. It assumes a scattering-dominated light transport, and it combines the scattering and the phase function in one parameter, called reduced scattering coefficient.

Slide 64

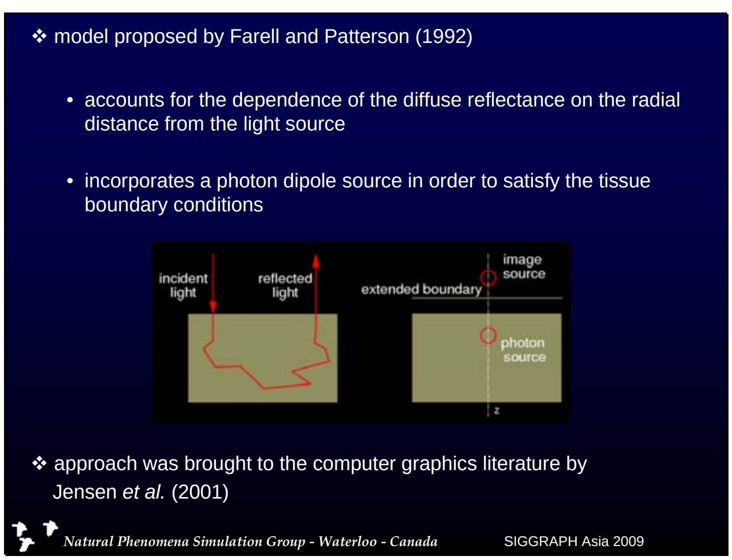

Slide 65

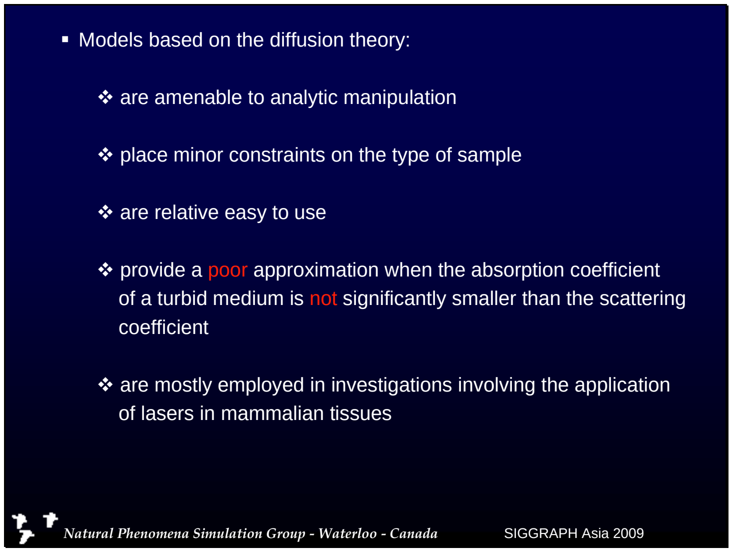

The diffusion approximation is applicable only under certain conditions. First, the measurement point needs to be remote from the light source, i.e., at a distance from the surface where the incident light beam has become completely diffuse [37]. Second, the absorption coefficient of the medium needs to be much smaller than its reduced scattering coefficient [18]. When the absorption coefficient of a turbid medium is not significantly smaller than the scattering coefficient, the diffusion theory provides a poor approximation for the photon transport equation [14,66,70,87].

Slide 66

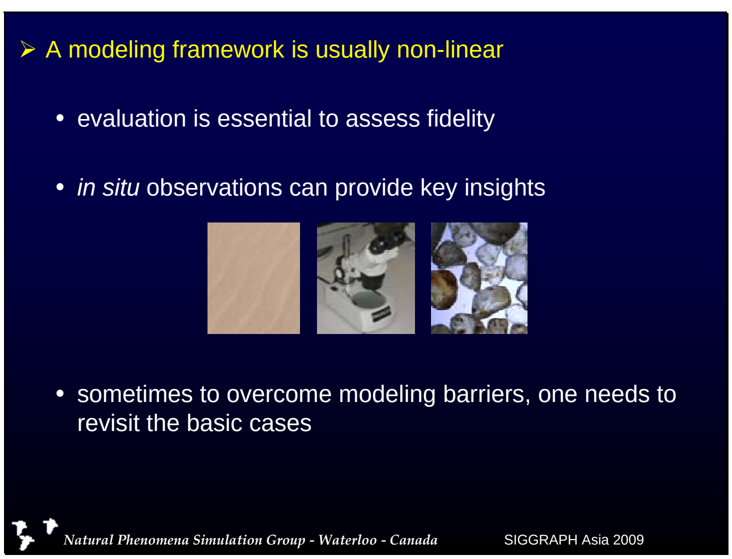

Slide 67

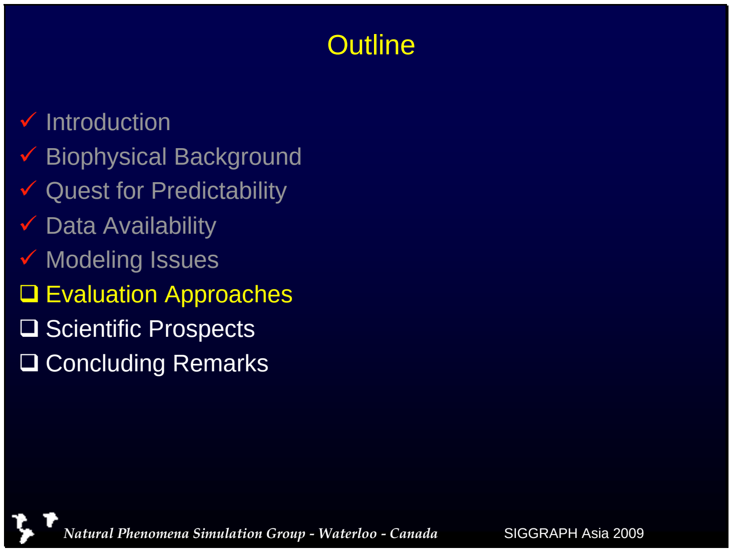

Slide 68

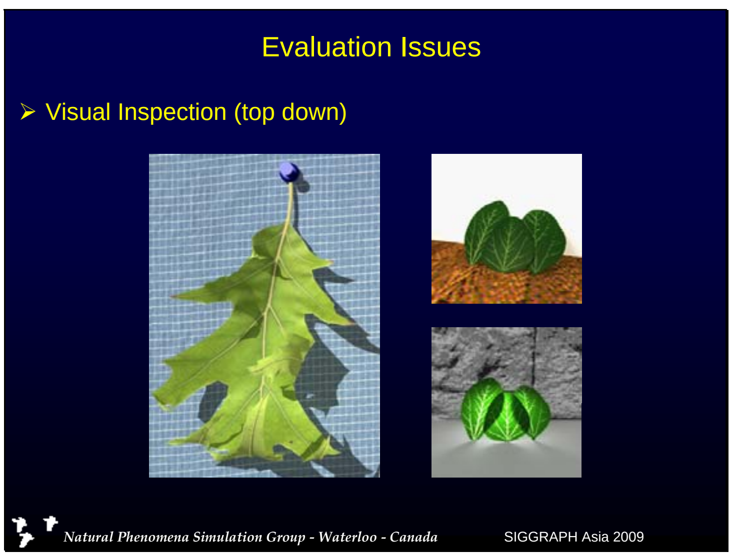

Slide 69

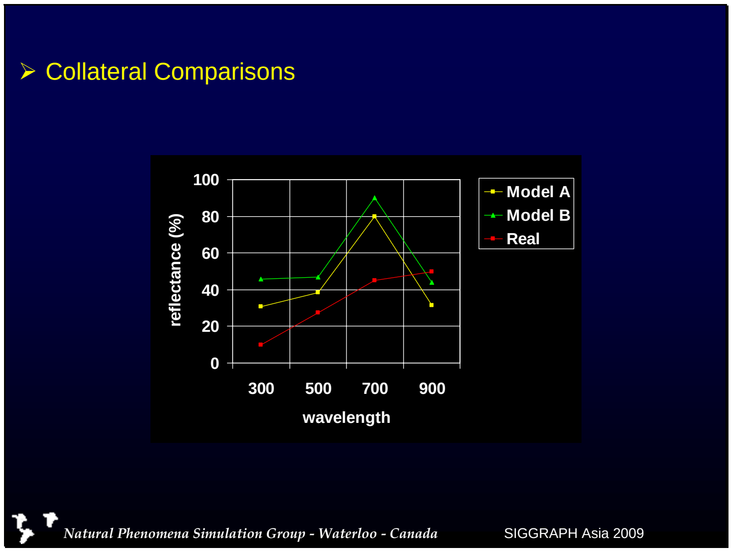

Slide 70

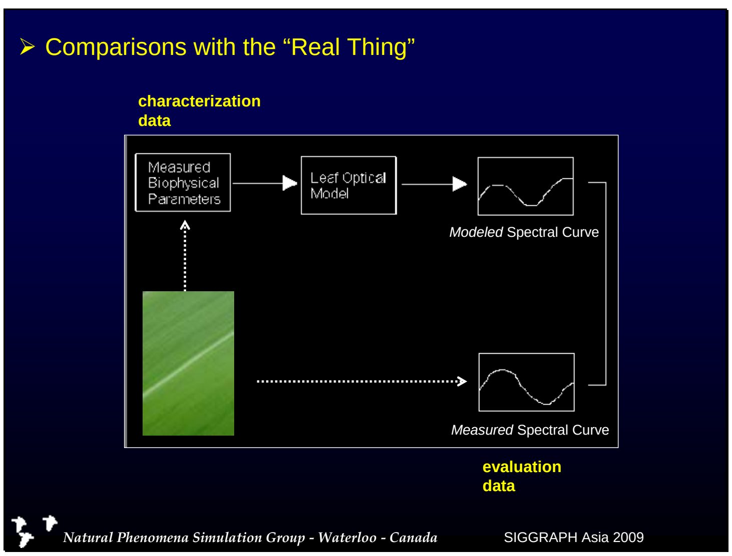

Modeled results can be obtained using virtual measurement devices. More specifically reflectance and transmittance curves can be obtained using virtual spectrophotometers [11], and BRDF and BTDF plots can be obtained using virtual goniophotometers [49].

Slide 71

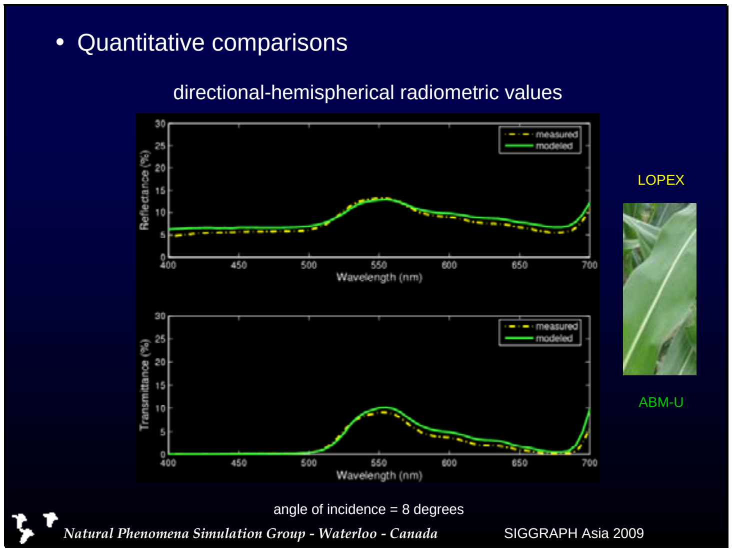

The ABM-U (algorithmic BDF (bidirectional scattering distribution function) model for unifacial leaves) was specifically designed to simulate light interactions with monocotyledonous (unifacial) leaves [1,3].

Slide 72

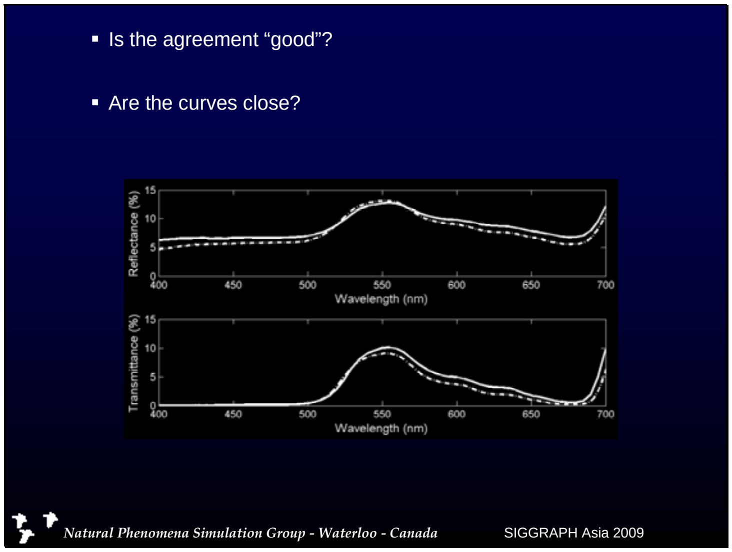

Slide 73

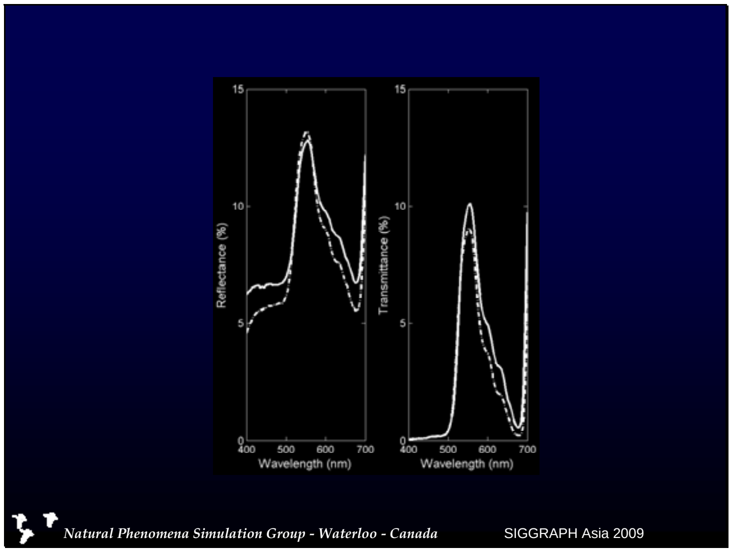

Slide 74

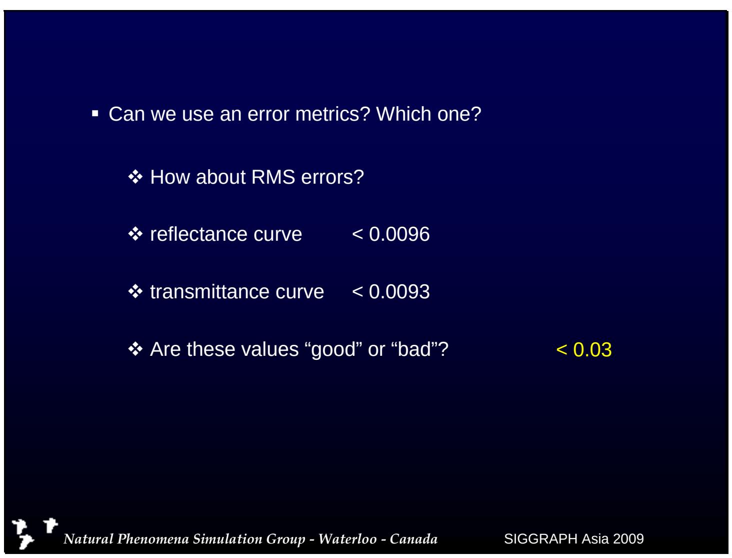

A RMS error lower than 0.03 is usually associated to good spectral reconstruction in the field of remote sensing of vegetation [42].

Slide 75

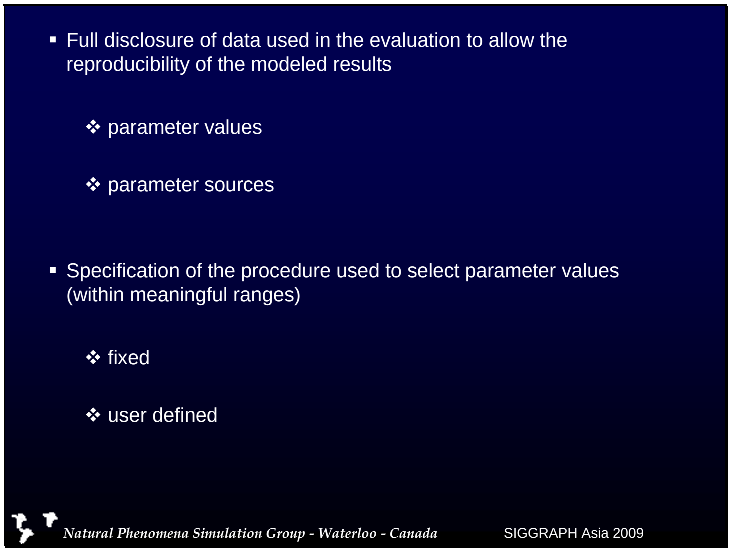

Slide 76

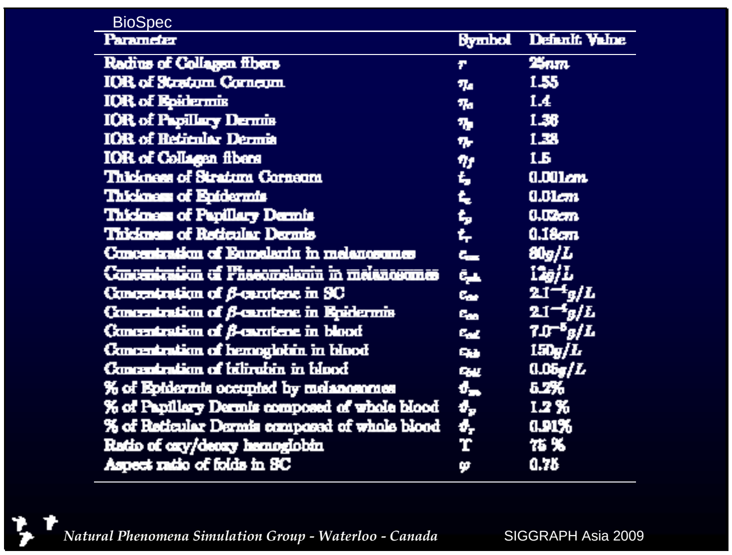
BioSpec

Parameter	Symbol	Default Value
Radius of Collagen fibers	r	$25nm$
IOR of Stratum Corneum	η_s	1.55
IOR of Epidermis	η_e	1.4
IOR of Papillary Dermis	η_p	1.36
IOR of Reticular Dermis	η_r	1.38
IOR of Collagen fibers	η_f	1.5
Thickness of Stratum Corneum	t_s	$0.001cm$
Thickness of Epidermis	t_e	$0.01cm$
Thickness of Papillary Dermis	t_p	$0.02cm$
Thickness of Reticular Dermis	t_r	$0.18cm$
Concentration of Eumelanin in melanosomes	c_{eu}	$80g/L$
Concentration of Phaeomelanin in melanosomes	c_{ph}	$12g/L$
Concentration of β-carotene in SC	$c_{\beta s}$	$2.1^{-4}g/L$
Concentration of β-carotene in Epidermis	$c_{\beta e}$	$2.1^{-4}g/L$
Concentration of β-carotene in blood	$c_{\beta d}$	$7.0^{-5}g/L$
Concentration of hemoglobin in blood	c_{hb}	$150g/L$
Concentration of bilirubin in blood	c_{bil}	$0.05g/L$
% of Epidermis occupied by melanosomes	ϑ_m	5.2%
% of Papillary Dermis composed of whole blood	ϑ_p	1.2 %
% of Reticular Dermis composed of whole blood	ϑ_r	0.91%
Ratio of oxy/deoxy hemoglobin	Υ	75 %
Aspect ratio of folds in SC	φ	0.75

For example, these are the parameters used to run BIOSPEC [48]. However, many of them are fixed, i.e., they correspond to biophysical properties which do not require user manipulation to match an individual's appearance attributes.

Slide 77

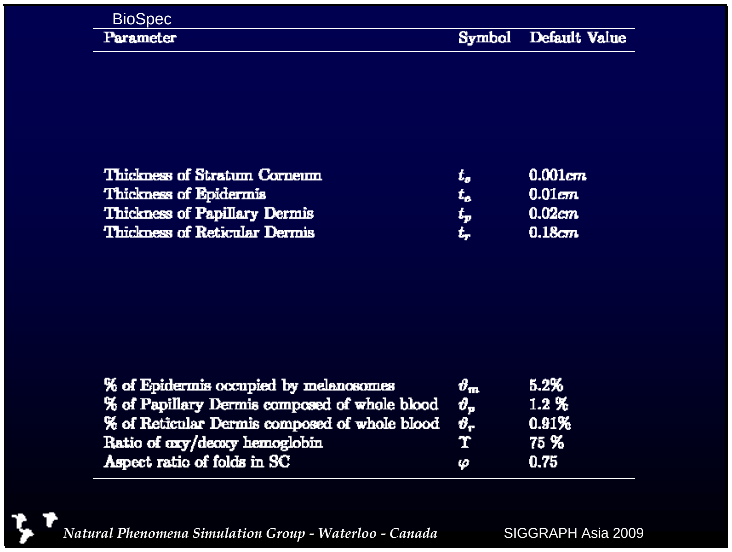

For example, the refractive indices of the tissues and the concentration of the pigments in these tissues correspond to average values available in the literature, and they are kept fixed for different specimens. However, if precise characterization data for a given specimen becomes available, they can be adjusted accordingly.

Slide 78

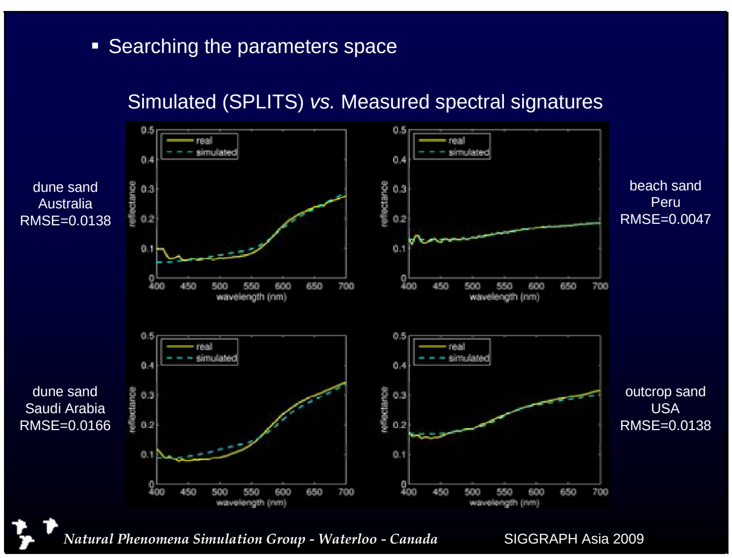

Slide 79

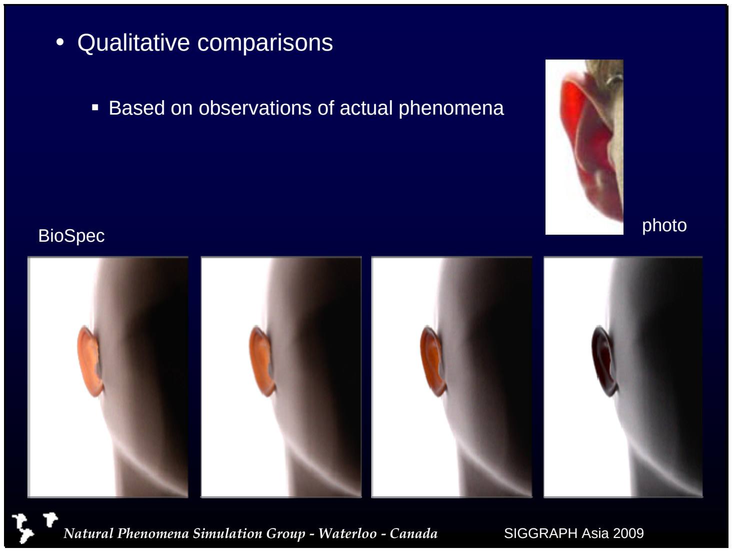

Slide 80

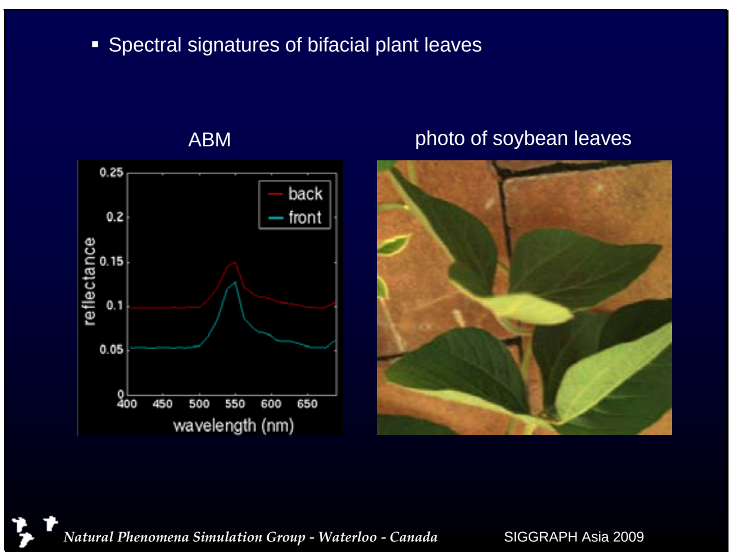

Slide 81

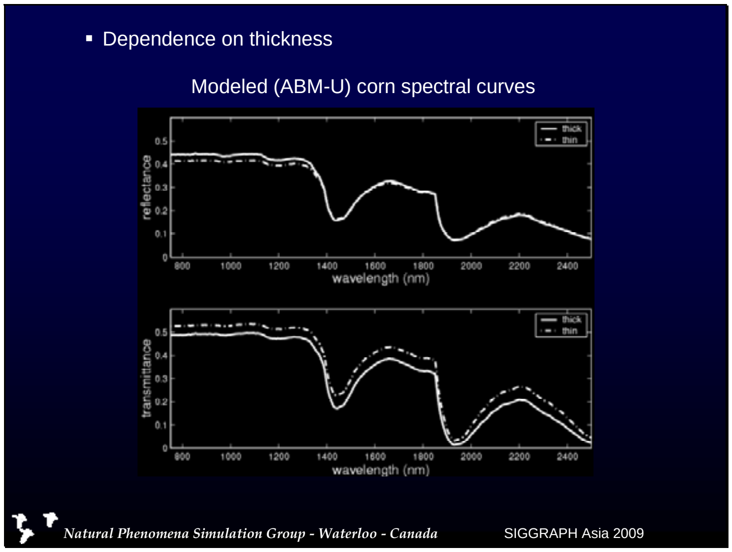

Experiments by Wooley [84] demonstrate that the reflectance of an unifacial leaf is not strongly dependent on the leaf thickness, within usual ranges, except for the near infrared domain from 750 to 1300 nm, where a thick unifacial leaf shows greater reflectance than a thin leaf. The transmittances, however, are more strongly influenced by the thickness of an unifacial leaf, with a thin unifacial leaf showing greater transmittance over the entire infrared domain. According to Wooley [84], the cause of these observed differences may be due to changes in internal arrangement of he tissues. These changes are related to the fact that unifacial leaves, such as corn leaves, shrank mostly in thickness. Thus, a reduction of their thickness, e.g., due to loss of water [85], without accompanying lateral shrinkage, can cause flattening of the mesophyll cells, which, in turn, may cause changes in the internal scattering profile of these leaves. The modeled results presented above demonstrate that the ABM-U [1,3] can reproduce this characteristic behavior observed in unifacial plant leaves line corn leaves.

Slide 82

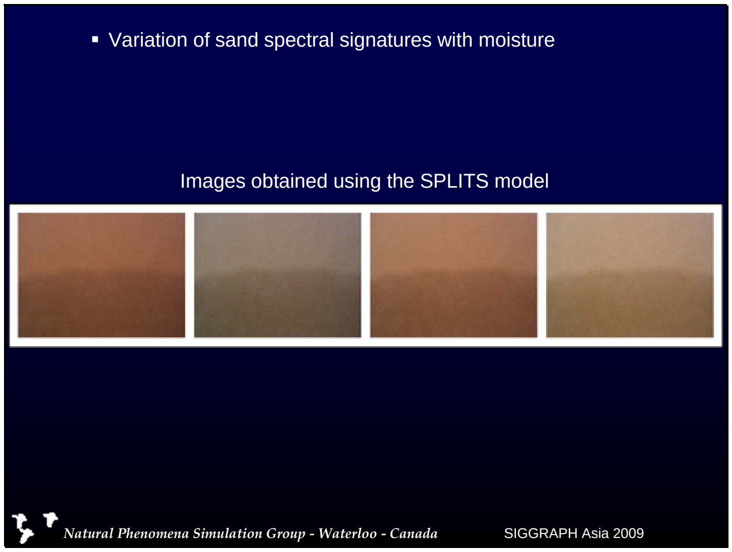

The water content in sand samples is usually expressed as the degree of saturation, denoted by *S*, which is the fraction of the pore space occupied by water [46,52].

Slide 83

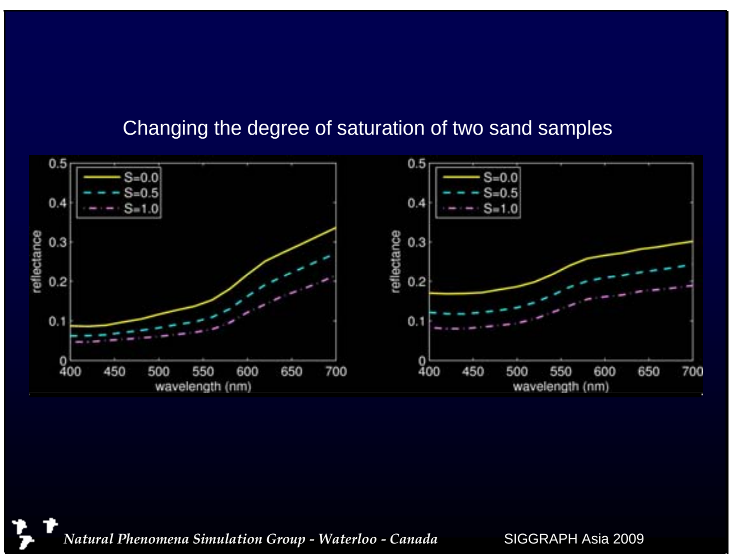

Slide 84

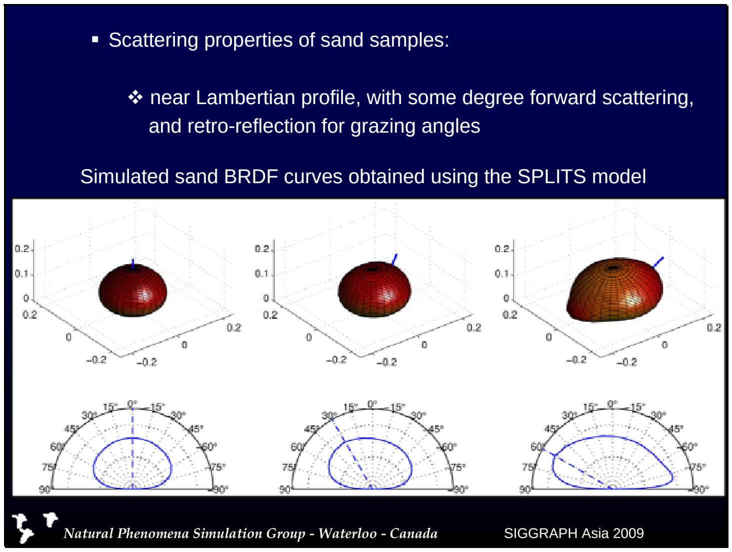

Sand reflects light in the forward direction, peaking at an larger angle to the normal than that of the direction of specular reflection [17]. In addition, it exhibits retro-reflection, which corresponds to reflection in the direction toward the light source [17]. The scattering simulations performed using SPLITS [47], as illustrated above, qualitatively reproduce these characteristics.

Slide 85

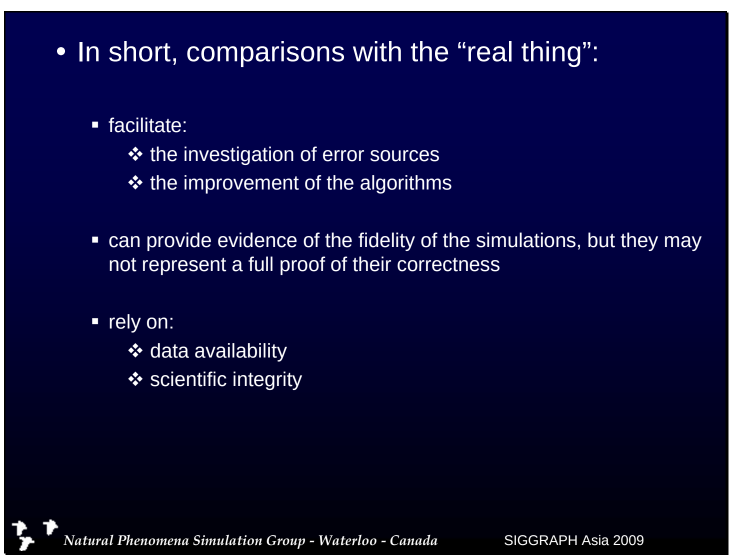

Slide 86

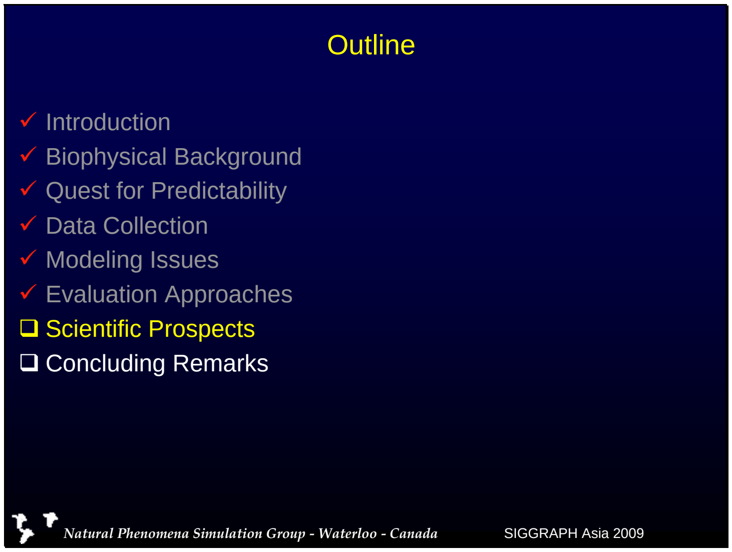

Slide 87

Slide 88

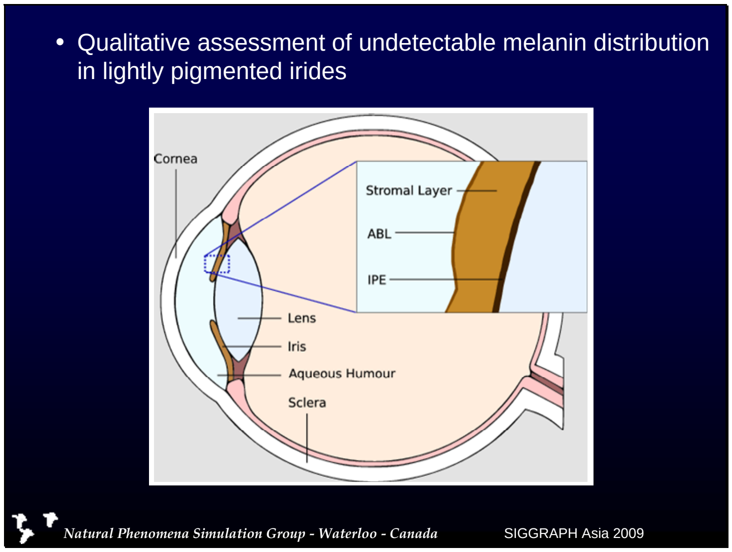

The iris can be described as a multilayered tissue stretching across the front of the eye. The outermost iridal layer is the anterior border layer (ABL). It consists of a dense arrangement of pigmented cells, collagen fibers, and fibroblasts [20]. Behind the ABL, we find the stromal layer (SL). Although both layers consist of connective tissue and pigmented cells, the SL is less dense than the ABL [20]. The SL is also characterized by the presence of loosely arranged collagen fibrils. The inner most layer is an opaque tissue called the iris pigment epithelium (IPE). It consists of heavily pigmented epithelial cells that are tightly fused by intercellular connections [39].

Measurements performed on blue irides using electron spin resonance spectroscopy detected less melanin in medium blue irides than in light blue irides [82]. It was postulated that this surprising finding could be related to the localization of pigment granules in the outermost iridal layers. Difficulties in performing separate wet measurements on the ABL and SL have precluded the *in loco* verification of this hypothesis, however [8].

Slide 89

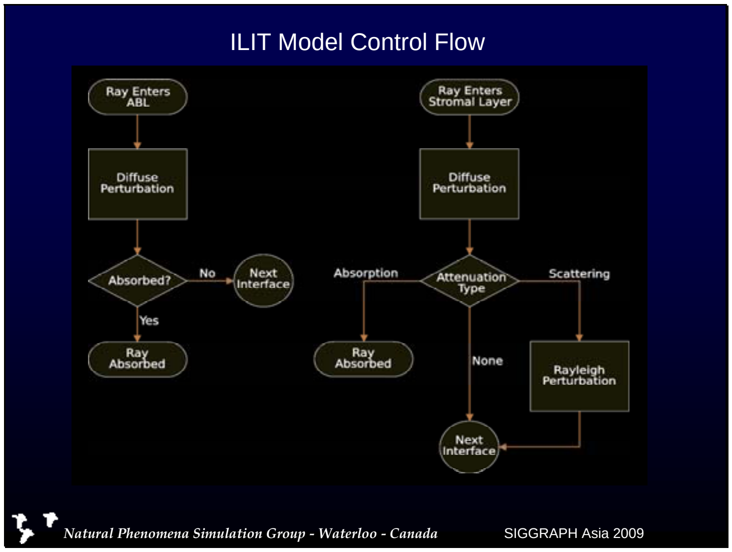

The ILIT model [50] uses ray optics and Monte Carlo methods to simulate light transport within the human iris.

Slide 90

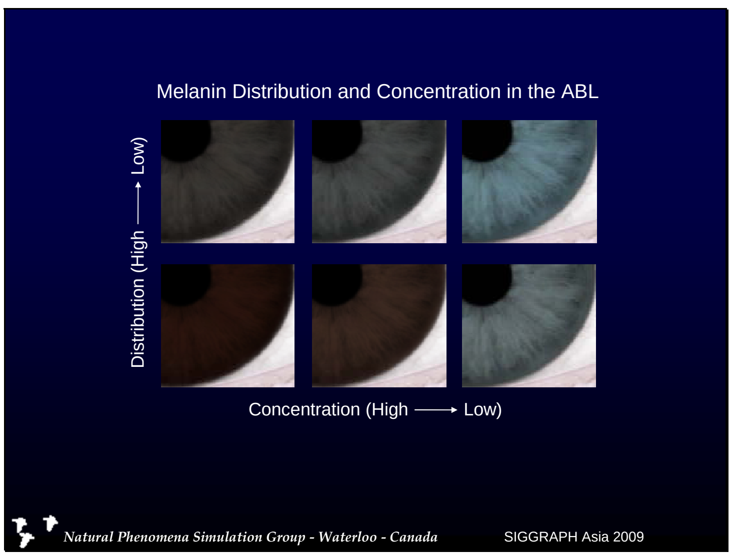

ILIT simulations [50] confirmed the assumption that brown irides have a darker appearance when most of the melanin present in the two outermost iridal layers, ABL and SL, are located in the former.

Slide 91

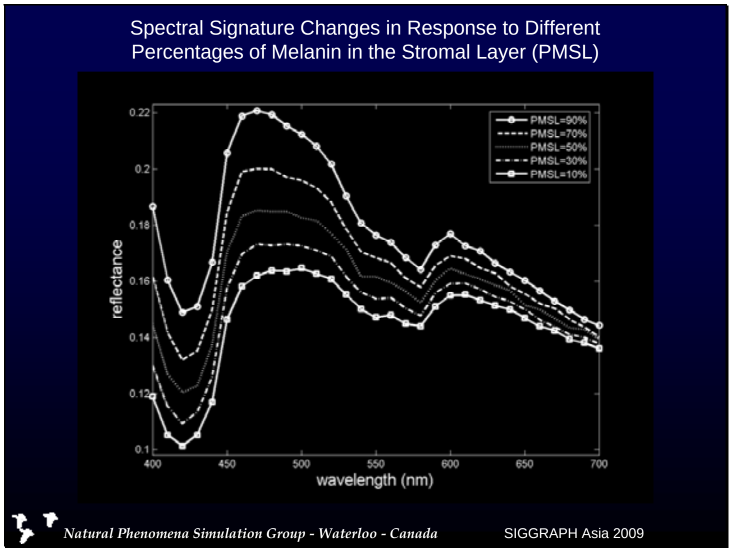

The results of ILIT simulations involving lightly pigmented irides [8], however, indicate a reverse relationship between the appearance of these specimens and their melanin distribution. The key biophysical parameter in these simulations is the ratio between the amount of melanin in the SL and the total amount of melanin in both ABL and SL, denoted by PMSL. As we increase the PMSL, the reflectance increases across the visible spectral domain (slide above), with reflectance values obtained at shorter wavelengths showing increase rates steeper than those associated to values obtained at longer wavelengths (slide below).

Slide 92

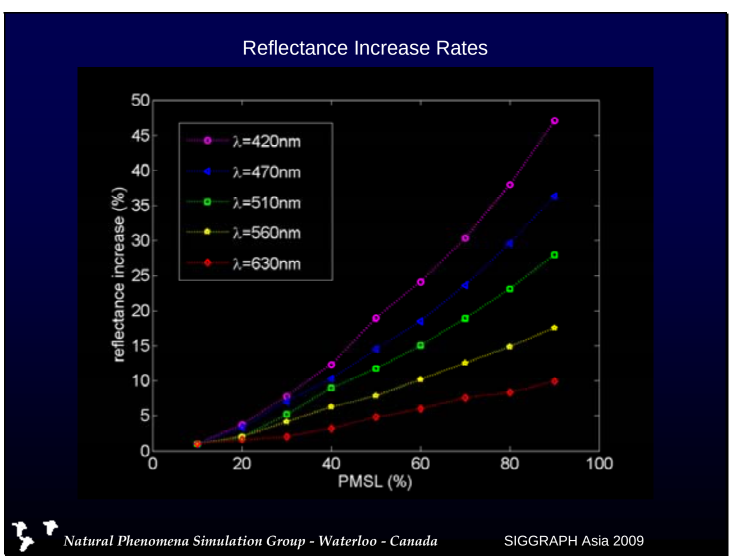

Slide 93

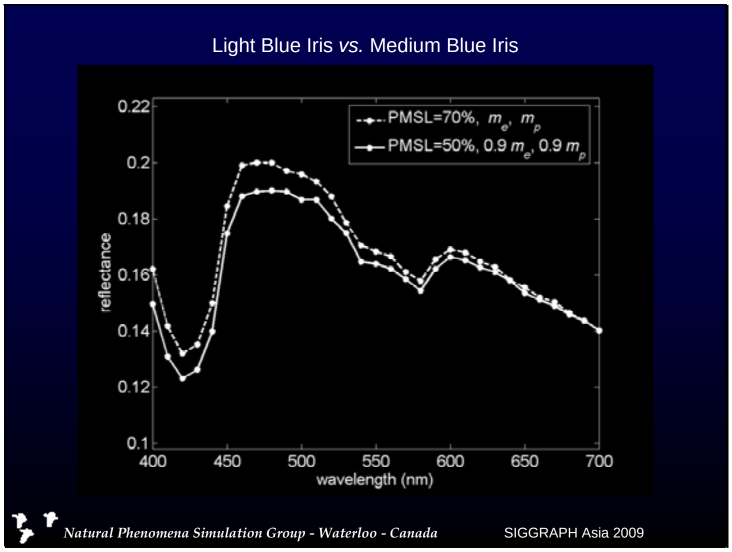

These changes suggest that the lighter shades and the hue transitions toward blue observed in lightly pigmented irides may be associated to a relatively higher content of melanin in the SL, which may be also related to existence of light blue irides with melanin contents higher than those measured for medium blue irides [82]. To illustrate the latter possibility, we performed another experiment [8] in which we considered two simulated lightly pigmented specimens A and B. For specimen A, we kept the same melanin amounts and set the PMSL to 70%. For specimen B, we reduced the melanin amounts in the ABL and SL by 10%, and we set the PMSL to 50%. The resulting spectral curves show a lower reflectance profile for specimen B despite the higher melanin content of specimen A.

Slide 94

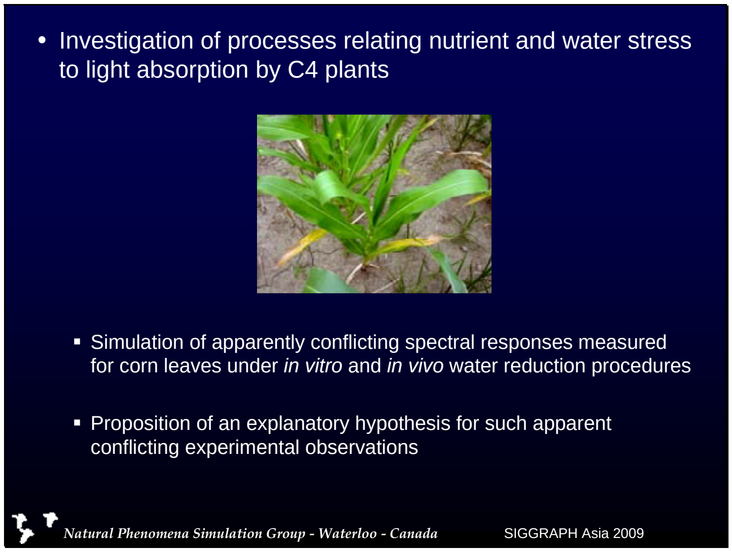

Due their increasing global demand (used not only for food, but also for fuel production), monocotyledonous C4 plants, such as maize (corn) and sugarcane, are becoming the focal point of studies involving the impact of abiotic stress factors on crop photosynthetic efficiency. Clearly, the availability of simulation tools specifically designed for these plants can contribute to expand the current understanding about their tolerance to less favorable environmental conditions. Furthermore, these tools can be used to assist the investigation of open questions involving their physiological responses to changes in water soil levels and the effects of limited nutrient and water supplies on their growing process [2]. From an agricultural and ecological point of view, one of the key benefits of performing *in silico* experiments using these tools is that such "virtual" experiments can provide quick feedback with respect to different strategies for increasing nutrient and water use efficiency of these crops given a set of possible environmental conditions [56].

Slide 95

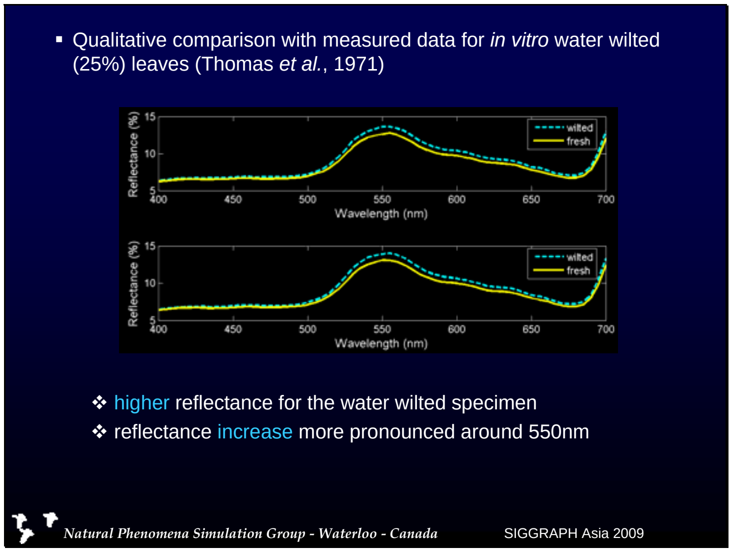

The modeled curves show a higher reflectance for the air-dried specimen in comparison with the fresh (turgid) specimen. This result is qualitatively consistent with the reflectance increase observed by Thomas et al. [73] in air-dried maize leaves whose water content was reduced by a similar amount (approximately 25%). Furthermore, it can be observed in the modeled curves that the reflectance increase is more pronounced in the region where the photosynthetic pigments have a lower absorptive capacity (centered at approximately 550nm). This feature is also noticeable in the actual measurements performed by Thomas et al. [73].

Slide 96

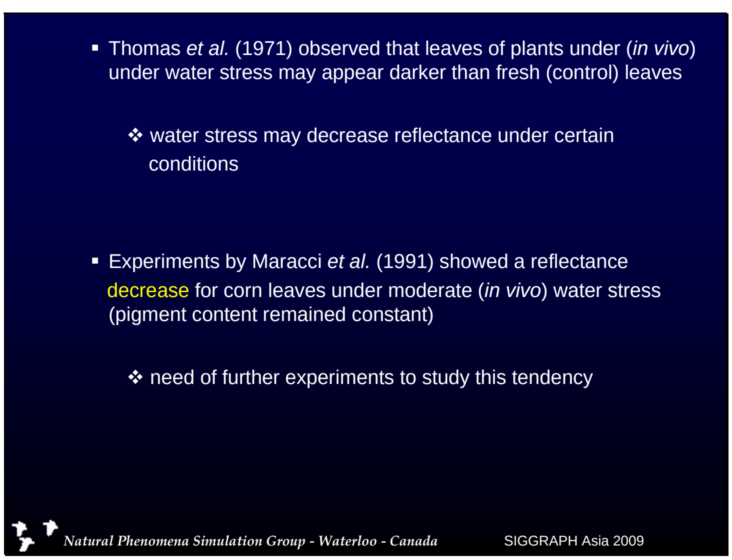

Slide 97

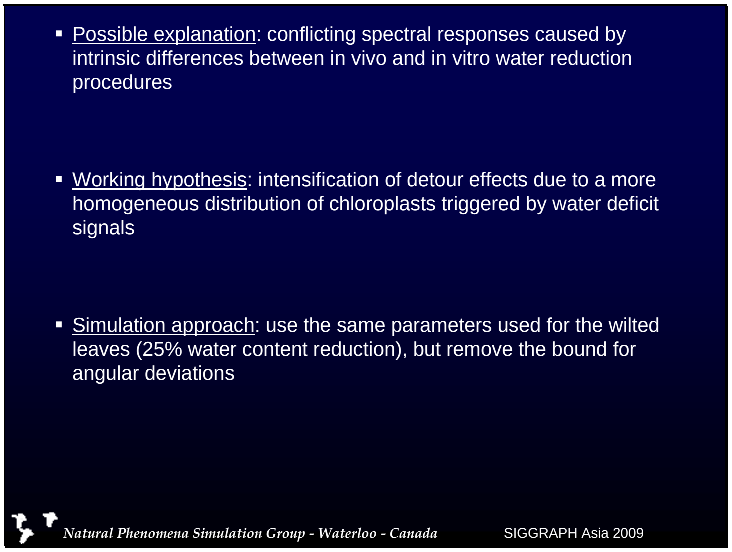

Slide 98

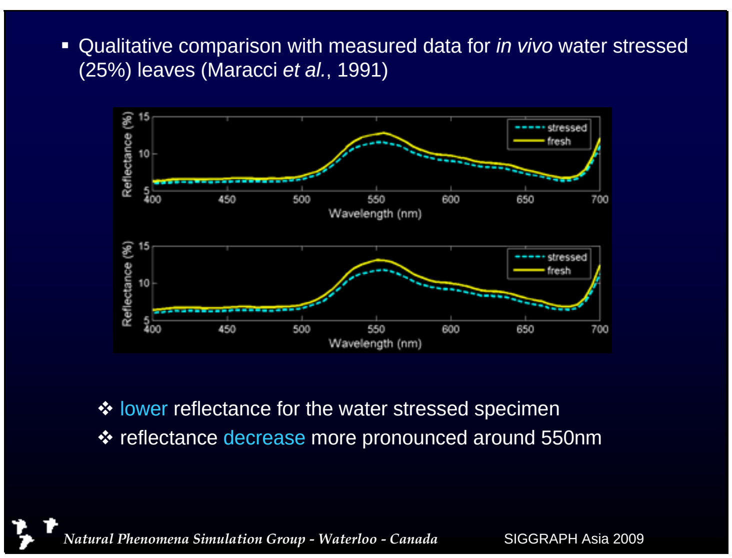

The results of these simulations show a lower overall reflectance for the *in vivo* water stressed specimen in comparison with the fresh (control) specimen. This reflectance decrease is qualitatively consistent with the observations made by Maracci et al. [53], and it is more pronounced in the region around 550nm, a feature also evident in their measurements.

Slide 99

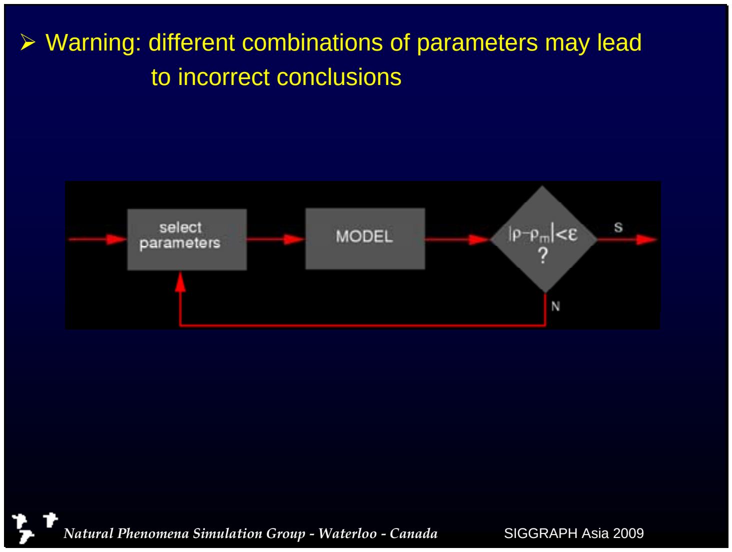

Slide 100

Slide 101

Outline

- ✓ Introduction
- ✓ Biophysical Background
- ✓ Quest for Predictability
- ✓ Data Availability
- ✓ Modeling Issues
- ✓ Evaluation Approaches
- ✓ Scientific Prospects
- ❑ Concluding Remarks

Natural Phenomena Simulation Group - Waterloo - Canada SIGGRAPH Asia 2009

Slide 102

Concluding Remarks

"… the idea is to try to give **all** of the information to help others to judge your contribution, not just the information that leads to judgment in one particular direction or another."

R.P. Feynman on the **principle of scientific integrity** (1974)

- ➢ Is this principle closely followed in practice?

Natural Phenomena Simulation Group - Waterloo - Canada SIGGRAPH Asia 2009

Slide 103

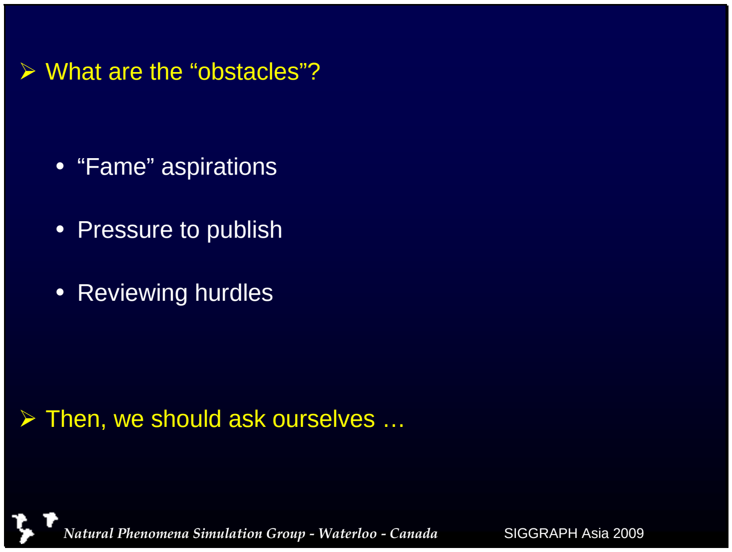

Slide 104

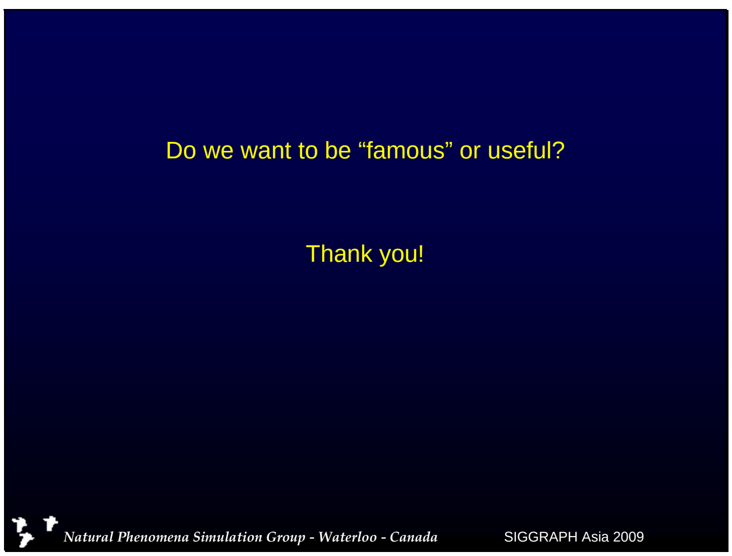

Slide 105

Credits: Diagrams, Images and Photos

- Denise Eng
- Jon Rokne
- Lesley Northam
- Bradley Kimmel
- Aravind Krishnaswamy
- Michael Lam
- Sung Min Hong
- Tenn Francis Chen
- Stephane Jacquemoud
- Adriane Baranoski
- Patricia Baranoski
- Gabriel Baranoski
- NASA